

# Copositive programming for mixed-binary quadratic optimization via Ising solvers

Robin Brown <sup>1, 2, 3</sup>, David E. Bernal Neira <sup>2,3</sup>, Davide Venturelli <sup>2,3</sup>, and Marco Pavone <sup>1</sup>

<sup>1</sup>Stanford University, Autonomous Systems Laboratory

<sup>2</sup>USRA Research Institute for Advanced Computer Science (RIACS)

<sup>3</sup>NASA Quantum Artificial Intelligence Laboratory (QuAIL)

July 28, 2022

## Abstract

Recent years have seen significant advances in quantum/quantum-inspired technologies capable of approximately searching for the ground state of Ising spin Hamiltonians. The promise of leveraging such technologies to accelerate the solution of difficult optimization problems has spurred an increased interest in exploring methods to integrate Ising problems as part of their solution process, with existing approaches ranging from direct transcription to hybrid quantum-classical approaches rooted in existing optimization algorithms. Due to the heuristic and black-box nature of the underlying Ising solvers, many such approaches have limited optimality guarantees. While some hybrid algorithms may converge to global optima, their underlying classical algorithms typically rely on exhaustive search, making it unclear if such algorithmic scaffolds are primed to take advantage of speed-ups that the Ising solver may offer. In this paper, we propose a framework for solving mixed-binary quadratic programs (MBQP) to global optimality using black-box and heuristic Ising solvers. We show the exactness of a convex copositive reformulation of MBQPs, which we propose to solve via a hybrid quantum-classical cutting-plane algorithm. The classical portion of this hybrid framework is guaranteed to be polynomial time, suggesting that when applied to NP-hard problems, the complexity of the solution is shifted onto the subroutine handled by the Ising solver.

## 1 Introduction

Recent years have seen significant advances in quantum and quantum-inspired Ising solvers, such as quantum annealers [1], quantum approximate optimization circuits [2], or coherent Ising machines [3]. These are devices/methodologies designed to solve optimization problems of the form:  $\min_{z \in \{-1, 1\}^n} \sum_{i,j} J_{i,j} z_i z_j + \sum_i h_i z_i$ , where  $J_{i,j}$ ,  $h_i$  are real coefficients and  $z_i \in \{-1, 1\}$  are discrete variables to be optimized over. The promise of leveraging such technologies to speed up the solution of complex optimization problems has spurred many researchers to explore how Ising solvers can be applied to problems in various domains. However, challenges in both hardware engineering and analysis of existing devices stand in the way of a crisp theoretical characterization of such solvers (e.g., optimality guarantees and speed-up in runtime) and they generally must be treated as heuristics.

A standard approach has emerged where an optimization problem is directly transcribed into an Ising problem, and the returned solution is taken at face value. Consequently, this method inherits the heuristic nature of the underlying Ising solver. While this may not be a limitation for many settings, it is insufficient for those requiring global optimality guarantees or provable bounds on solution quality.

As an alternative, a few authors have proposed decomposition methods based on the Alternating Direction Method of Multipliers (ADMM), [4], or Benders Decomposition (BD), [5, 6, 7]. Critically, when ADMM is applied to non-convex problems, it is not guaranteed to converge. When it does, it is often to a local optimum without guarantees on gaps to global optimality. On the other hand, while it may be possible to derive optimality guarantees using BD, proving convergence typically relies on an exhaustive search through the “complicating variables”. This makes it unclear whether such an algorithmic scaffold is primed to take advantage of speed-ups that the Ising solver may offer.

**Contributions** Our work is motivated by the desire to extend existing work to applications that require global optimality guarantees. We set the standard for designing a hybrid quantum-classical optimization algorithm that offers resilience to the heuristic nature of Ising solvers while taking advantage of any speed-up they may offer. Specifically, we envision convergent hybrid quantum-classical algorithms that (1) use Ising solvers as a primitive with limited requirements on/knowledge of their optimality guarantees and (2) have polynomial complexity in the classical portions of the algorithm. To this end, the contribution of this paper is an algorithmic framework that satisfies these key desiderata. Concretely,

1. We revisit and extend a result of [8] and show that there is an exact convex formulation of many mixed-binary quadratic optimization problems as a copositive program. Neglecting the challenges of working with copositive matrices, convex programs are a well-understood class of optimization problems with a wide variety of efficient solution algorithms. By reformulating mixed-binary quadratic programs as copositive programs, we open the door for hybrid-quantum classical algorithms that are based on existing convex optimization algorithms.
2. To solve the copositive programs, we propose a novel hybrid quantum-classical optimization algorithm based on cutting-plane algorithms, a well-established class of convex optimization algorithms. We show that the complexity of the portion of the algorithm handled by the classical computer has polynomial scaling. This analysis suggests that when applied to NP-hard problems, the complexity of the solution is shifted onto the subroutine handled by the Ising solver.
3. We conducted benchmarking based on the maximum clique problem to validate our theoretical claims and evaluate potential speed-ups from using a stochastic Ising solver in lieu of a state-of-the-art deterministic solver or an Ising heuristics. Results indicate that the Ising formulation of the subproblems of the hybrid algorithm is efficient versus a MILP formulation in `Gurobi`, and the hybrid algorithm is competitive even against a non-hybridized Ising formulation of the full problem solved by simulated annealing.

While preparing this manuscript, a hybrid classical-quantum method relying upon a Frank-Wolfe method was published [9]. This work also leverages a similar copositive reformulation of quadratic binary optimization problems. We highlight the differences between that work and the one in our manuscript below. This manuscript considers the optimization problem class of mixed-binary quadratic programs, while in [9], the authors propose their method for quadratic binary optimization problems, a subcase of the problems considered herein. Moreover, we provide proof of the exactness and strong duality for copositive/completely positive optimization stemming from the mixed-integer quadratic reformulation, addressing an open question in the field. In their manuscript, [9] conjectures the results proved in this manuscript to be true. Finally, our solution method, which is based on cutting-plane algorithms, has a potential exponential speed-up in run-time compared to Frank-Wolfe algorithms.

## 1.1 Related Work

One dominant method for mapping optimization problems into Ising problems is through direct transcription. This process typically involves discretizing continuous variables and passing constraints into the objective through a penalty function; the returned solution is often taken at face value or with minimal post-processing to enforce feasibility. Owing to its simplicity, this process has found applications in a variety of problems including jobshop scheduling [10], routing problems [11], community detection [12], and all of Karp’s 21 NP-complete models [13], among others. Critically, this approach is unforgiving of the heuristic and imperfect characteristics of existing and near-term devices. This approach is often justified by the statement that a good quality solution is sufficient for many problem settings; however, there are also many practical problems where guarantees or bounds on optimality are paramount, such as neural network verification [14], refinery pooling, phase and chemical equilibrium [15], among others. Even with experimental efforts attesting to the quality of returned solutions, it is unclear to what degree such results can be extrapolated to problem classes or instances that have not been evaluated.

As an alternative to direct transcription, there is a burgeoning body of literature exploring the potential of decomposition methods for designing hybrid quantum-classical algorithms. These generally refer to algorithms that divide effort between a classical and quantum computer, with each

computer informing the computation carried out by the other. Among these, algorithms based on the Benders Decomposition (BD) are gaining traction. BD is particularly effective for problems characterized by “complicating variables”, for which the problem becomes easy once these variables are fixed. For example, a mixed-integer linear program (MILP) becomes a linear program (LP) once the integer variables are fixed—the integers are the complicating variables. BD iterates between solving a master problem over the complicating variables and sub-problems where the complicating variables are fixed, whose solution is used to generate cuts for the master problem. Both [5] and [6] consider mixed-integer programming (MIP) problems where the integer variables are linked to the continuous variables through a polyhedral constraint and leverage a reformulation where dependence on the continuous variables is expressed as constraints over the extreme rays and points of the original feasible region. Because the number of extreme rays and points may be exponentially large, the constraints are not written down in full but iteratively generated from the solutions of the sub-problems. The master problem is an integer program consisting of these constraints and is solved using the quantum computer. Notably, the generated constraint set may be large, with the worst case being the generation of the entire constraint set, resulting in a large number of iterations. The approach in [7] attempts to mitigate this by generating multiple cuts per iteration and selecting the most informative subset of these cuts. Instead of using the quantum computer to solve the master problem, the quantum computer is used to heuristically select cuts based on a minimum set cover or maximum coverage metric. While this may effectively reduce the number of iterations and size of the constraint set, the master problem is often an integer program that may be computationally intractable. For each of the proposed approaches, it is unclear how the complexity of the problem is distributed through the solution process—for example, for [5, 6] the complexity might show up in the number of iterations and for [7] it might show up when solving the master problem. Consequently, it is ambiguous whether BD-based approaches can take advantage of a speed-up in the Ising solver, even if one were to exist.

Another decomposition that has been explored is based on the Alternating Direction Method of Multipliers (ADMM)[4]. This is an algorithm to decompose large-scale optimization problems into smaller, more manageable sub-problems [16]. While originally designed for convex optimization, ADMM has shown great success as a heuristic for non-convex optimization as well, [17], and significant progress has been made towards explaining its success in such settings [18]. In [4], the authors propose an ADMM-based decomposition with three sub-problems: the first being over just the binary variables, the second being the full problem with a relaxed copy of the binary variables, and the third being a term that ties the binary variables and their relaxed copies together. For quadratic pure-binary problems, the authors show that the algorithm converges to a stationary point of the augmented Lagrangian, which may not be a global optimizer—convergence to a global optimum is only guaranteed under the more stringent Kurdyka-Łojasiewicz conditions on the objective function [19]. Unfortunately, the assumptions guaranteeing convergence to a stationary point fail in the presence of continuous variables.

A third class of decomposition proposed and implemented in D-Wave’s `qbsolv` solver is based on tabu search [20]. `qbsolv` can be seen as iterating between a large-neighborhood local search (using an Ising solver) and tabu improvements to locally refine the solution (using a classical computer), where previously found solutions are removed from the search space in each iteration. During the local search phase, subsets of the variables are jointly optimized while the remaining variables are fixed to their current values. The solution found in this phase is then used to initialize the tabu search algorithm, and the process is repeated for a fixed number of iterations. Critically, it is unclear whether the algorithm is guaranteed to converge and, if so, what its optimality guarantees are. While finite convergence of tabu search is investigated in [21], it relies on either recency or frequency memory that ensures an exhaustive search of all potential solutions.

Another approach for purely integer programming problems is based on the computation of a Graver basis through the computation of the integer null-space of the constraint set as proposed in [22]. This null-space computation is posed as a quadratic unconstrained binary optimization (QUBO) and then post-processed to obtain the Graver basis of the constraint set, a test-set of the problem. The test-set provides search directions for an augmentation-based algorithm. For a convex objective, it provides a polynomial oracle complexity in converging to the optimal solution. The authors initialize the problem by solving a feasibility-based QUBO and extend this method to non-convex objectives by allowing multiple starting points for the augmentation. The multistart procedure also alleviates the requirement for computing the complete Graver basis of the problem, which grows exponentially with the problem’s size. Considering an incomplete basis or non-convex objectives makes the Graver Augmentation Multistart Algorithm (GAMA) a heuristic for general integer programming problems

and cannot address problems with continuous variables.

In this paper, we seek to fill a gap in the literature on rigorous solution methods for mixed-integer non-convex optimization problems that use Ising solvers as a subroutine. By elucidating the hidden convex structure of non-convex problems, we pave the way for hybrid quantum-classical algorithms based on efficient convex optimization algorithms. We show that a hybrid algorithm based on cutting-plane algorithms inherits their convergence guarantees without sacrificing efficiency.

## 1.2 Quantum/Quantum-inspired Ising Solvers

Adiabatic quantum computing (AQC) is a quantum computation paradigm that operates by initializing a system in the ground state of an initial Hamiltonian and slowly sweeping the system to an objective Hamiltonian. This Hamiltonian, referred to as the cost Hamiltonian, maps the objective function of the classical Ising model onto a system with as many quantum bits, or qubits, as original variables in the Ising model. The adiabatic theorem of quantum mechanics states that if the system evolution is “sufficiently slow”, the system ends up in the ground state of the desired Hamiltonian. Here, “sufficiently slow” depends on the minimum energy gap between the ground and the first excited state throughout the system evolution [23]. Since the evaluation of the minimal gap is mostly intractable, one is forced to phenomenologically “guess” the evolution’s speed, and if it is too fast, the undesired non-adiabatic transitions can occur. Additionally, real devices are plagued with various incarnations of physical noise, such as thermal fluctuations or decoherence effects, that can hamper computation. The situation is further exacerbated by the challenge of achieving dense connectivity between qubits—densely connected problems are embedded in devices by chaining together multiple physical qubits to represent one logical qubit. The heuristic computational paradigm that encompasses these additional noise and non-quantum effects is known as Quantum Annealing (QA)— [24] provides a review on QA with a focus on possible routes towards solving the open questions in the field.

An alternative paradigm to AQC is the gate-based model of quantum computing. Within the gate-based model, Variational Quantum Algorithms (VQAs) is a class of hybrid quantum-classical algorithms that can be applied to optimization [25]. VQAs share a common operational principle where the “loss function” of a parameterized quantum circuit is measured on a quantum device and evaluated on a classical processor, and a classical optimizer is used to update (or “train”) the circuit’s parameters to minimize the loss. VQAs are often interpreted as a quantum analog to machine learning, leaving many similar questions open regarding their trainability, accuracy, and efficiency.

The quantum approximate optimization algorithm (QAOA) is a specific instance of a VQA where the structure of the quantum circuit is the digital analog of adiabatic quantum computing [2]. QAOA operates by alternating the application of the cost Hamiltonian and a mixing Hamiltonian; the number of alternating blocks is referred to as the circuit depth. For each one of the alternating steps, either mixing or cost application, a classical optimizer needs to determine how long each step should be performed, encoded as rotation angles. Optimizing the expected cost function with respect to the rotation angles is a continuous low-dimensional non-convex problem. QAOA is designed to optimize cost Hamiltonians, such as the ones derived from classical Ising problems. Performance guarantees can be derived for QAOA with well-structured problems, given that the optimal angles are found in the classical optimization step. Although approximation guarantees have not been derived for arbitrary cost Hamiltonians, even depth-one QAOA circuits have non-trivial performance guarantees for specific problems and cannot be efficiently simulated on classical computers [26], thus bolstering the hope for a speed-up in near-term quantum machines. Moreover, the algorithm’s characteristics, such as relatively shallow circuits, make it amenable to be implemented in currently available noisy intermediate-scale quantum (NISQ) computers compared to other algorithms requiring fault-tolerant quantum devices [27], not yet developed to the best of the authors’ knowledge. While QAOA’s convergence to optimal solutions is known to improve with increased circuit depth and to succeed in the infinite depth limit following its equivalence to AQC, its finite depth behavior has remained elusive due to the challenges in analyzing quantum many-body dynamics and other practical complications such as decoherence when implementing long quantum circuits, compilation issues, and hardness of the optimal angle classical problem [28]. Even considering these complications, QAOA has been extensively studied and implemented in current devices [29, 30], becoming one of the most popular alternatives to address combinatorial optimization problems modeled as Ising problems using gate-based quantum computers. Several other Quantum heuristics for Ising problems have been proposed, usually requiring fault-tolerant Quantum computers. We direct the interested reader to a recent

review on the topic [31].

An alternative physical system for solving Ising problems that has emerged is coherent Ising machines (CIMs), which are optically pumped networks of coupled degenerate optical parametric oscillators. As the pump strength increases, the equilibrium states of an ideal CIM correspond to the Ising Hamiltonian’s ground states encoded by the coupling coefficients. Large-scale prototypes of CIMs have achieved impressive performance in the lab, thus driving theoretical study of their fundamental operating principles. While significant advances have been made on this front, we still lack a clear theoretical understanding of the CIMs’ computational performance. Since a thorough understanding of the CIM is limited by our capacity to prove theorems about complex dynamic systems, near-term usage of CIMs must treat them as a heuristic rather than a device with performance guarantees [32]. Even so, there are empirical observations that in many cases, the median complexity of solving Ising problems using CIM scales as  $\exp \sqrt{N}$  where  $N$  is the size of the problem [33], making it a potential approach to solve these problems efficiently in practice.

We note that there are other types of Ising machines, including classical thermal annealers (based on spintronics, optics, memristors, and digital hardware accelerators), dynamical-systems solvers (based on optics and electronics), and superconducting-circuit quantum annealers. We direct the interested reader to [33], which provides a recent review and comparison of various methods for constructing Ising machines and their operating principles.

While there is optimism regarding improvements to and our understanding of quantum technology in the coming decades, it is still unclear what their impact will be in the near term. We believe that the method presented in this paper is a complementary approach to algorithm design that meets these technological advancements “halfway”. In particular, we envision a class of hybrid quantum-classical optimization algorithms that, with limited knowledge of or requirements on the guarantees of any particular Ising solver, can transform black-box solutions to ones with rigorous optimality while simultaneously benefiting from any advantage that does exist.

**Organization** In Section 2, we present notation, terminology, and the problem setting covered by our approach. In Section 3, we introduce the proposed framework, including convex reformulation via copositive programming, a high-level overview of cutting-plane algorithms, and a specific discussion of their application to copositive programming. Section 4 provides numerical experiments supporting our assertions about the proposed approach. Finally, we conclude and highlight future directions in Section 5.

## 2 Preliminaries

### 2.1 Notation and Terminology

In this paper, we solely work with vectors and matrices defined over the real numbers and reserve lowercase letters for vectors and uppercase letters for matrices. We will also follow the convention that a vector  $x \in \mathbb{R}^n$  is to be treated as a column vector, i.e., equivalent to a matrix of dimension  $n \times 1$ . For a matrix  $M$ , we use  $M_{i,j}$  to denote the entry in the  $i$ th row and  $j$ th column,  $M_{i,*}$  denotes the entire  $i$ th row, and  $M_{*,j}$  denotes the entire  $j$ th column. We use  $\mathbf{1}$  to denote the all-ones vectors and  $\mathbf{1}_{\{j\}}$  to denote the  $j$ th standard basis vector (i.e., a vector where all entries are zero except for a 1 for the  $j$ th entry). The  $p$ -norm of a vector  $v \in \mathbb{R}^n$  is defined as  $\|v\|_p := (\sum_{i=1}^n v_i^p)^{1/p}$ . We reserve the letter  $I$  to denote the identity matrix. For two matrices,  $M$  and  $N$ , we use  $\langle M, N \rangle = \text{Tr}(M^\top N)$  to denote the matrix inner product. Note that for two vectors,  $\text{Tr}(x^\top y) = x^\top y$  because  $x^\top y$  is a scalar, so the matrix inner product is consistent with the standard inner product on vectors. For sets,  $S_M + S_N := \{M + N \mid M \in S_M, N \in S_N\}$  is their Minkowski sum,  $S_M \cup S_N$  their union, and  $S_M \cap S_N$  their intersection. For a cone,  $\mathcal{K}$ , its dual cone is defined as  $\mathcal{K}^* = \{X \mid \langle X, K \rangle \geq 0, \forall K \in \mathcal{K}\}$ . While we work with matrix cones in this paper, this definition of dual cones is consistent with vector cones as well. In this paper, the two cones we will work with are the cone of completely positive matrices and the cone of copositive matrices. The cone of completely positive (CP) matrices,  $C^*$ , is the set of matrices that have a factorization with entry-wise non-negative entries:

$$C_n^* := \{X \in \mathbb{R}^{n \times n} \mid X = \sum_k x^{(k)}(x^{(k)})^\top, \quad x^{(k)} \in \mathbb{R}_{\geq 0}^n\} \quad (1)$$

The cone of copositive matrices,  $\mathcal{C}$ , is the set of matrices defined by:

$$\mathcal{C}_n := \{X \in \mathbb{R}^{n \times n} \mid v^\top X v \geq 0, \quad \forall v \in \mathbb{R}_{\geq 0}^n\} \quad (2)$$

As suggested by the notation, the cones of completely positive and copositive matrices are duals of each other.

In this paper, we will use the terms Ising problem and quadratic unconstrained binary optimization (QUBO) interchangeably. An Ising problem is an optimization problem of the form:  $\min_{z \in \{-1, 1\}^n} \sum_{i,j} J_{i,j} z_i z_j + \sum_i h_i z_i$ , where  $J_{i,j}, h_i$  are real coefficients and  $z_i \in \{-1, 1\}$  are discrete variables to be optimized over. A QUBO, which is an optimization problem of the form  $\min_{x \in \{0, 1\}^n} \sum_{i,j} Q_{i,j} x_i x_j$  can be reformulated as an Ising problem using the change of variable  $z = 2x - \mathbb{1}$ . This translates to coefficients in the Ising problem  $J_{i,j} = \frac{1}{4} Q_{i,j}$ ,  $h_i = \frac{1}{2} \sum_j Q_{i,j}$ , and a constant offset of  $\frac{1}{4} \sum_{i,j} Q_{i,j}$ .

## 2.2 Problem Setting

In this paper, we consider mixed-binary quadratic programs (MBQP) of the form:

$$\begin{aligned} & \underset{x \in \mathbb{R}^n}{\text{minimize}} && x^\top Q x + 2c^\top x \\ & \text{subject to} && Ax = b, \quad A \in \mathbb{R}^{m \times n}, b \in \mathbb{R}^m, \\ & && x \geq 0, \\ & && x_j \in \{0, 1\}, \quad j \in B \end{aligned} \quad (\text{MBQP})$$

where the set  $B \subseteq \{1, \dots, n\}$  indexes which of the  $n$  variables are binary. This is a general class of problems that encompasses problems including QUBOs, standard quadratic programming, the maximum stable set problem, and the quadratic assignment problem. Because mapping to an Ising problem can also be equivalently expressed as a QUBO, many problems tackled with Ising solvers thus far pass through a formulation similar to the form of Problem (MBQP). Using the result in [8, Sec. 3.2], the formulation considered in this paper can be extended to include constraints of the form  $x_i x_j = 0$  that force at least one of  $x_i$  or  $x_j$  to be zero, i.e., *complementarity constraints*. For ease of notation, this extension is left out of the present discussion.

## 3 Proposed Methodology

In this section, we will discuss our proposed methodology for solving Problem (MBQP) with optimality guarantees given access to heuristic/black-box Ising solvers. Our result relies on a convex reformulation of Problem (MBQP) as a copositive program. Leveraging convexity, we propose to solve the problem using cutting-plane algorithms. These belong to a broad class of convex optimization algorithms whose standard components give rise to a natural separation between the role of the Ising solver versus a classical computer.

We first state Burer's exact reformulation of Problem (MBQP) as a completely positive program and its dual copositive program. We then show that under mild conditions (i.e., feasibility and boundedness) of the original MBQP, the copositive and completely positive programs exhibit strong duality. We will then introduce the class of cutting-plane algorithms and summarize the complexity guarantees of several well-known variants. Finally, we explicitly show how cutting-plane algorithms can be used to solve copositive optimization problems given a copositivity oracle and discuss how to implement a copositivity oracle using an Ising solver.

### 3.1 Convex formulation as a copositive program

In his seminal work, Burer showed that MBQPs can be represented exactly as completely positive programs of the form:

$$\begin{aligned}
& \text{minimize} && \left\langle \begin{pmatrix} Q & c \\ c^\top & \cdot \end{pmatrix}, \begin{pmatrix} X & x \\ x^\top & 1 \end{pmatrix} \right\rangle \\
& X \in \mathbb{R}^{n \times n}, x \in \mathbb{R}^n && \\
& \text{subject to} && \left\langle \begin{pmatrix} \cdot & \frac{1}{2}A_{i,*}^\top \\ \frac{1}{2}A_{i,*} & \cdot \end{pmatrix}, \begin{pmatrix} X & x \\ x^\top & 1 \end{pmatrix} \right\rangle = b_i, \quad i = 1, \dots, m, \\
& && \left\langle \begin{pmatrix} A_{i,*}^\top A_{i,*} & \cdot \\ \cdot & \cdot \end{pmatrix}, \begin{pmatrix} X & x \\ x^\top & 1 \end{pmatrix} \right\rangle = b_i^2, \quad i = 1, \dots, m, \\
& && \left\langle \begin{pmatrix} -\mathbf{1}_{\{j\}} \mathbf{1}_{\{j\}}^\top & \frac{1}{2} \mathbf{1}_{\{j\}} \\ \frac{1}{2} \mathbf{1}_{\{j\}}^\top & \cdot \end{pmatrix}, \begin{pmatrix} X & x \\ x^\top & 1 \end{pmatrix} \right\rangle = 0, \quad j \in B, \\
& && \begin{pmatrix} X & x \\ x^\top & 1 \end{pmatrix} \in \mathcal{C}_{n+1}^*,
\end{aligned} \tag{CPP}$$

where exactness means that Problems (MBQP) and (CPP) have the same optimal objective and for an optimal solution,  $(x^*, X^*)$ , of (CPP),  $x^*$  lies within the convex hull of optimal solutions for (MBQP) [8, Theorem 2.6]. Similar to semi-definite programming (SDP) relaxations, the completely positive formulation involves lifting to a matrix variable representing first and second-degree monomials of the variables in (MBQP), making the objective function and constraints linear. Unlike SDP relaxations, however, the complete positivity constraint is sufficient for ensuring that the feasible region of (CPP) is exactly the convex hull of the feasible region of (MBQP). This distinction is what ensures that the optimal value of (CPP) is exactly that of (MBQP), whereas for an SDP relaxation, the optimal solution may lie outside of the convex hull resulting in a lower objective value (i.e., a *relaxation gap*).

Taking the dual of (CPP) yields a copositive optimization problem of the form [34, Section 5.9]:

$$\begin{aligned}
& \text{maximize} && \gamma + \sum_{i=1}^m \mu_i^{(\text{lin})} b_i + \mu_i^{(\text{quad})} b_i^2 \\
& \mu, \lambda, \gamma && \\
& \text{subject to} && M(\mu, \lambda, \gamma) \in \mathcal{C}_{n+1},
\end{aligned} \tag{COP}$$

where

$$\begin{aligned}
M(\mu, \lambda, \gamma) := & \begin{pmatrix} Q & c \\ c^\top & \cdot \end{pmatrix} - \sum_{i=1}^m \mu_i^{(\text{lin})} \begin{pmatrix} \cdot & \frac{1}{2}A_{i,*}^\top \\ \frac{1}{2}A_{i,*} & \cdot \end{pmatrix} - \sum_{i=1}^m \mu_i^{(\text{quad})} \begin{pmatrix} A_{i,*}^\top A_{i,*} & \cdot \\ \cdot & \cdot \end{pmatrix} \\
& - \sum_{j \in B} \lambda_j \begin{pmatrix} -\mathbf{1}_{\{j\}} \mathbf{1}_{\{j\}}^\top & \frac{1}{2} \mathbf{1}_{\{j\}} \\ \frac{1}{2} \mathbf{1}_{\{j\}}^\top & \cdot \end{pmatrix} - \gamma \begin{pmatrix} \cdot & \\ & 1 \end{pmatrix}
\end{aligned} \tag{3}$$

is a parametrized linear combination of the constraint matrices. The dual copositive program has a linear objective and a single copositivity constraint—this is a convex optimization problem. While weak duality always holds between an optimization problem and its dual, strong duality is not generally guaranteed. Showing that strong duality holds is critical for ensuring convergence of specific optimization algorithms and exactness when solving the dual problem as an alternative to solving the primal.

**Theorem 3.1** (Strong Duality). *If Problem (MBQP) is feasible with bounded feasible region, then strong duality holds between Problems (CPP) and (COP) (i.e.,  $\min(\text{CPP}) = \max(\text{COP})$ ).*

*Proof Sketch.* Our proof proceeds by first showing strong duality between the alternative representation of (CPP) (using a homogenized formulation of the equality constraints) and its dual. By showing that the optimal value of (COP) is lower-bounded by the optimal value of this homogenized dual problem, we can sandwich the optimal values of Problems (CPP) and (COP) by those of a primal-dual pair that has been shown to exhibit strong duality. The complete proof of this result is provided in Appendix 6.1.  $\square$

In prior work, characterization of the duality gap between Problems (CPP) and (COP) has remained elusive because the feasible region of Problem (CPP) never has an interior, thus prohibiting straightforward application of Slater’s constraint qualification. This result is significant because it shows that under mild conditions, the copositive formulation is exact. This means that the optimal values of Problems (MBQP) and (COP) are equivalent, so solving Problem (COP) is a valid alternative to solving Problem (MBQP). Moreover, the optimal solution of Problem (CPP) can be recovered

from the optimal solution of Problem (COP) by optimizing the Lagrangian function with respect to the optimal dual variables [35, Prop 5.3.3].

While Problems (CPP) and (COP) are both convex, neither resolve the difficulty of Problem (MBQP) as even checking complete positivity (resp. copositivity) of a matrix is NP-hard (resp. co-NP-complete) [36]. Instead, they should be viewed as “packaging” the complexity of the problem entirely in the copositivity/complete positivity constraint. There are a number of classical approaches for (approximately) solving copositive/completely positive programs directly, such as the sum of squares hierarchy [37, 38], feasible descent method in the completely positive cone, approximations of the copositive cone by a sequence of polyhedral inner and outer approximations, among others [39, 40, 41]. In this paper, we will exploit the innate synergy between checking copositivity, which is most naturally posed as a quadratic minimization problem, and solving Ising problems. This perspective is suggestive of a hybrid quantum-classical approach where the quantum computer is responsible for checking feasibility (i.e., the “hard part”) of the copositive program while the classical computer directs the search towards efficiently reducing the search space.

### 3.2 Cutting-Plane/Localization Algorithms

Cutting-plane/localization algorithms are convex optimization algorithms that divide labor between checking feasibility—abstracted as a *separation oracle*—and optimization of the objective. In this section, we provide a high-level overview of each algorithmic step and summarize both the run-time and oracle complexities of several well-known variants; these complexity measures will ultimately correspond to the complexity of the sub-routine handled by the classical computer and the number of calls to the Ising solver, respectively.

While cutting-plane algorithms are often used to solve both constrained and unconstrained optimization problems, they are generally evaluated in terms of their complexity when solving the *feasibility problem*.

**Definition 1** (Feasibility Problem). *For a set of interest  $S \subset \mathbb{R}^m$ , which can only be accessed through a separation oracle, the feasibility problem is concerned with either finding a point in the set  $x \in S$  or proving that  $S$  does not contain a ball of radius  $r$ .*

**Definition 2** (Separation Oracle). *A separation oracle for a set  $S$ ,  $\text{Oracle}_S(\cdot)$  takes as input a point  $x \in \mathbb{R}^m$  and either returns **True** if  $x \in S$  or a separating hyperplane if  $x \notin S$ . A separating hyperplane is defined by a vector,  $a \in \mathbb{R}^m$  and scalar  $b \in \mathbb{R}$  such that  $a^\top s \leq b$  for all  $s \in S$  but  $a^\top x \geq b$ .*

The feasibility problem formulation is non-restrictive because these methods can be readily adapted to solving quasi-convex optimization problems with only a simple modification to the separation oracle. In particular, if the separation oracle indicates feasibility and returns a vector  $g$  where  $f(y) < f(x)$  implies that  $g^\top y \geq g^\top x$ , this serves as a separating hyperplane for the subset of the feasible region that has a better objective than the test point. If  $f$  is subdifferentiable, any subgradient  $g \in \partial f(x)$  satisfies this condition, and for Problem (COP) choosing  $g$  as the objective’s coefficient vector is sufficient.

Although there are many variations of cutting-plane algorithms, at a high level, they follow a standard template that consists of alternating between checking feasibility of a test point, updating an outer approximation of the feasible region, and judiciously selecting the next test point. This standard template is summarized in Algorithm 1. By choosing subsequent test points to be the center of the outer approximation, the algorithm is guaranteed to make consistent progress in reducing the search space (where the metric of progress may also vary across cutting-plane algorithms). Intuitively, cutting plane algorithms can be considered a high-dimensional analog of binary search.

A number of well-known variants of cutting-plane algorithms are summarized in Table 1. Differences across instantiations of cutting-plane algorithms vary in how subsequent test points are chosen, how the outer approximation is updated, and how progress in decreasing the outer approximation’s size is measured. Each of the surveyed variants strikes a different balance between the computational effort needed to compute a good center versus the resolution used to represent the outer approximation. Critically, except for the Center of Gravity method, all cutting-plane algorithms summarized in Table 1 have a polynomial complexity in the dimension of the optimization variables in terms of both oracle queries and total run-time excluding the oracle calls (i.e., the total complexity of adding the cuts and generating test points). This suggests that if a cutting-plane algorithm were applied to Problem (COP), the complexity of the problem is offloaded onto the separation oracle—this is the subroutine we propose to handle using an Ising solver.



---

**Algorithm 1:** Cutting-plane meta-algorithm (feasibility problem)

---

**Input:**  $S_0 \subseteq \mathbb{R}^m$  (Initial Set) with  $\text{Vol}(S_0) \leq R$   
**Output:**  $x \in S$  or **False** if  $S$  does not contain a ball of volume  $r$   
 $x \leftarrow \text{Center}(S_0);$   
 $k \leftarrow 0;$   
**while** *Oracle*( $x$ ) is not *True* and  $\text{Vol}(S_k) \geq r$  **do**  
     $S_{k+1} \leftarrow \text{Add\_Cut}(S_k, \text{Oracle}(x));$   
     $x \leftarrow \text{Center}(S_{k+1});$   
     $k \leftarrow k + 1;$   
**end**  
**if** *Oracle*( $x$ ) is *True* **then**  
    **return**  $x;$   
**else**  
    **return** *False*;  
**end**

---

Name	Oracle Queries	Total Run-time (excluding oracle queries)	References
Center of Gravity	$\mathcal{O}(m \log(\frac{R}{r}))$	#P-hard [42]	[43]
Ellipsoid	$\mathcal{O}(m^2 \log(m \frac{R}{r}))$	$\mathcal{O}(m^4 \log(m \frac{R}{r}))$	[44, 45, 46]
Inscribed Ellipsoid	$\mathcal{O}(m \log(m \frac{R}{r}))$	$\mathcal{O}((m \log(m \frac{R}{r}))^{4.5})$	[47, 48]
Volumetric Center	$\mathcal{O}(m \log(m \frac{R}{r}))$	$\mathcal{O}(m^{1+\omega} \log(m \frac{R}{r}))$	[49]
Analytic Center	$\mathcal{O}(m \log^2(m \frac{R}{r}))$	$\mathcal{O}(m^{1+\omega} \log^2(m \frac{R}{r}) + (m \log(m \frac{R}{r}))^{2+\frac{\omega}{2}})$	[50]
Random Walk	$\mathcal{O}(m \log(m \frac{R}{r}))$	$\mathcal{O}(m^7 \log(m \frac{R}{r}))$	[51]
Lee, Sidford, Wong	$\mathcal{O}(m \log(m \frac{R}{r}))$	$\mathcal{O}(m^3 \log^{\mathcal{O}(1)}(m \frac{R}{r}))$	[52]

Table 1: This table summarizes the number of oracle queries and total run-time guarantees of a number of well-known cutting-plane variants. The stated run-times are in terms of the problem dimension,  $m$ , the volume of the initial set,  $R$ , and the minimum volume of the set of interest,  $r$ . The constant  $\omega$  stands for the fast matrix multiplication constant.

### 3.3 Application to copositive optimization

Now that we have introduced cutting-plane algorithms, we are in a position to discuss their application to the copositive program (COP). First, we will show how a *copositivity oracle* can be readily transformed into a separation oracle for the feasible region of Problem (COP). We will conclude with a discussion of how a copositivity oracle can be implemented using an Ising solver. Formally, we define a copositivity oracle as follows:

**Definition 3** (Copositivity Oracle). *A copositivity oracle takes as input a matrix,  $M$ , and either returns **True** if  $M$  is copositive or returns a vector  $z \in \mathbb{R}_{\geq 0}^n$  such that  $z^\top M z < 0$  (a “certificate of non-copositivity”).*

A copositivity oracle can be turned into a separation oracle for the feasible region of Problem (COP) by expanding the terms in  $z^\top M(\hat{\mu}, \hat{\lambda}, \hat{\gamma})z$ . Explicitly, a test point,  $(\hat{\mu}, \hat{\lambda}, \hat{\gamma})$ , is infeasible if and only if  $M(\hat{\mu}, \hat{\lambda}, \hat{\gamma})$  is not copositive. Given  $M(\hat{\mu}, \hat{\lambda}, \hat{\gamma})$  as input, the copositivity oracle returns a certificate of non-copositivity  $z \in \mathbb{R}_{\geq 0}^{n+1}$  such that  $z^\top M(\hat{\mu}, \hat{\lambda}, \hat{\gamma})z < 0$ . In contrast, feasibility means

that  $z^\top M(\mu, \lambda, \gamma)z \geq 0$ . Equivalently, the halfspace defined by

$$b = z^\top \begin{pmatrix} Q & c \\ c^\top & \cdot \end{pmatrix} z, \quad (4)$$

$$a[\mu_i^{(\text{lin})}] = z^\top \begin{pmatrix} \cdot & \frac{1}{2}A_{i,*}^\top \\ \frac{1}{2}A_{i,*} & \cdot \end{pmatrix} z, \quad (5)$$

$$a[\mu_i^{(\text{quad})}] = z^\top \begin{pmatrix} A_{i,*}^\top A_{i,*} & \cdot \\ \cdot & \cdot \end{pmatrix} z, \quad (6)$$

$$a[\lambda_j] = z^\top \begin{pmatrix} -\mathbb{1}_{\{j\}} \mathbb{1}_{\{j\}}^\top & \frac{1}{2} \mathbb{1}_{\{j\}} \\ \frac{1}{2} \mathbb{1}_{\{j\}}^\top & \cdot \end{pmatrix} z, \quad (7)$$

$$a[\gamma] = z^\top \begin{pmatrix} \cdot \\ \cdot \\ 1 \end{pmatrix} z, \quad (8)$$

is a separating hyperplane for  $(\hat{\mu}, \hat{\lambda}, \hat{\gamma})$ , where we use symbolic indexing to explicitly denote which variable each coefficient corresponds to. Explicitly, the inner product between  $a$  and  $(\mu, \lambda, \gamma)$  is given by

$$a^\top(\mu, \lambda, \gamma) = \sum_i a[\mu_i^{(\text{lin})}] \mu_i^{(\text{lin})} + \sum_i a[\mu_i^{(\text{quad})}] \mu_i^{(\text{quad})} + \sum_j a[\lambda_j] \lambda_j + a[\gamma] \gamma. \quad (9)$$

This shows that given a copositivity oracle, constructing a separation oracle for Problem (COP) entails evaluating  $\mathcal{O}(m)$  vector-matrix-vector products, each of dimension  $\mathcal{O}(n)$ . The cutting-plane algorithms presented in Section 3.2 can then be applied without further modification.

Checking copositivity of  $M(\mu, \lambda, \gamma)$  is naturally posed as solving the following (possibly non-convex) quadratic minimization problem

$$\begin{aligned} & \underset{z \in \mathbb{R}_{\geq 0}^{n+1}}{\text{minimize}} && z^\top M(\mu, \lambda, \gamma)z \\ & \text{subject to} && \|z\|_p \leq 1, \end{aligned} \quad (10)$$

where a matrix is copositive if and only if  $\min(10)$  is non-negative<sup>1</sup>. There are several alternative approaches for checking copositivity [53, 54, 55, 56, 57]; however, they are typically derived with Problem (10) as the starting point and designed to exploit particular properties of Problem (10). By choosing  $p = \infty$ , Problem (10) can be approximated by a QUBO where an approximation of the matrix  $M$ ,  $\hat{M}$ , is used such that the optimization variables  $\hat{z}$  represent a binary expansion of  $z$  with  $k$  bits as follows:

$$\begin{aligned} & \underset{\hat{z}}{\text{minimize}} && \hat{z}^\top \hat{M}(\mu, \lambda, \gamma) \hat{z} \\ & \text{subject to} && \hat{z} \in \{0, 1\}^{k(n+1)}. \end{aligned} \quad (\text{QUBO})$$

Explicitly,  $\hat{M}(\mu, \lambda, \gamma)$  and  $M(\mu, \lambda, \gamma)$  are related as follows:

$$\hat{M}(\mu, \lambda, \gamma) = \mathcal{D}^\top M(\mu, \lambda, \gamma) \mathcal{D}, \quad (11)$$

where

$$\mathcal{D} := \begin{pmatrix} \frac{1}{2^0} & \cdots & \frac{1}{2^{k-1}} & 0 & \cdots & 0 & \cdots & 0 & \cdots & 0 \\ 0 & \cdots & 0 & \frac{1}{2^0} & \cdots & \frac{1}{2^{k-1}} & \cdots & 0 & \cdots & 0 \\ \vdots & \vdots & \vdots & \vdots & \vdots & \vdots & \vdots & \vdots & \vdots & \vdots \\ 0 & \cdots & 0 & 0 & \cdots & 0 & \cdots & \frac{1}{2^0} & \cdots & \frac{1}{2^{k-1}} \end{pmatrix}. \quad (12)$$

The construction of (QUBO) is detailed in Appendix 6.2. The explicit implementation of `Oracle(·)` is summarized in Algorithm 2. Critically, the constraints of (10) are implied by the natural domain of the Ising solver, mitigating the need to tune coefficients in a penalty method carefully.

### 3.4 Discussion

In summary, we propose to solve Problem (MBQP) by constructing the equivalent copositive formulation in (COP) and applying any variant of Algorithm 1. Within Algorithm 1, the implementation of `Oracle(·)` is specified by Algorithm 2. This process is depicted in Figure 1. Now that we have presented our method in full, several comments are in order.

<sup>1</sup>While copositivity is defined as a condition over all of  $\mathbb{R}_{\geq 0}^{n+1}$ , quadratic scaling of the objective ensures that optimizing over a norm ball is sufficient for detecting copositivity.

---

**Algorithm 2:** Separation oracle,  $\text{Oracle}(\cdot)$ 


---

**Input:**  $(\hat{\mu}, \hat{\lambda}, \hat{\gamma})$  (Test point)

**Output:**

$$\begin{cases} \text{True} & \text{if } (\hat{\mu}, \hat{\lambda}, \hat{\gamma}) \text{ is feasible} \\ \text{Separating hyperplane for } (\hat{\mu}, \hat{\lambda}, \hat{\gamma}) & \text{otherwise} \end{cases}$$

// Solve (QUBO) using an Ising solver

$$z^* \leftarrow \arg \min_{\hat{z}} \quad (\text{QUBO})$$

if  $\min(\text{QUBO}) \geq 0$  then

    return *True*;

else

$$z = \mathcal{D}z^* \tag{13}$$

$$b = z^\top \begin{pmatrix} Q & c \\ c^\top & \cdot \end{pmatrix} z \tag{14}$$

$$a[\mu_i^{(\text{lin})}] = z^\top \begin{pmatrix} \cdot & \frac{1}{2}A_{i,*}^\top \\ \frac{1}{2}A_{i,*} & \cdot \end{pmatrix} z \tag{15}$$

$$a[\mu_i^{(\text{quad})}] = z^\top \begin{pmatrix} A_{i,*}^\top & \cdot \\ \cdot & \cdot \end{pmatrix} z \tag{16}$$

$$a[\lambda_j] = z^\top \begin{pmatrix} -\mathbf{1}_{\{j\}} \mathbf{1}_{\{j\}}^\top & \frac{1}{2} \mathbf{1}_{\{j\}} \\ \frac{1}{2} \mathbf{1}_{\{j\}}^\top & \cdot \end{pmatrix} z \tag{17}$$

$$a[\gamma] = z^\top \begin{pmatrix} \cdot \\ \cdot \\ 1 \end{pmatrix} z \tag{18}$$

    return  $a, b$ ;

end

---

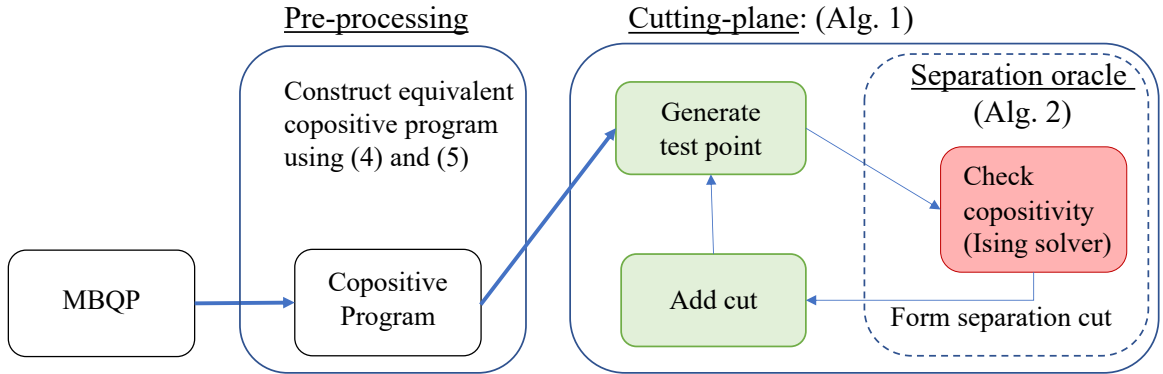


Figure 1: This figure depicts the entire solution process for solving a MBQP of the form (MBQP).

**Computational complexity** While the stated complexity of the cutting-plane algorithms is applicable to any problem, it is suggestively stated in terms of the variable  $m$ . This notational overload is a deliberate choice because the dimension of the dual copositive program is equal to the total number of constraints in Problem (CPP), which is  $2m + |B| + 1 = \mathcal{O}(m)$ . The number of constraints can be reduced to  $m + |B| + 1$  using the homogenized completely positive reformulation presented in Appendix 6.1—while this will have no impact on the asymptotic complexity of the method, it can result in a practical reduction in run-time. If  $\mathcal{T}_Q$  represents the oracle complexity of a particular method, the additional overhead of converting the copositivity oracle into a separation oracle is given by  $\mathcal{O}(mn^2\mathcal{T}_Q)$ .

**Discretization size** Discretization of the copositivity check automatically introduces an approximation to the copositivity checks. The approximation fidelity is improved as the number of discretization points is increased, although it is limited by the hardware. Not only does representing a finer discretization require more qubits, but it also results in a greater skew in the coefficients of the Ising Hamiltonian—this becomes challenging since many existing hardware platforms have limited precision in their implementable couplings. In contrast, too coarse of a discretization runs the risk of missing the certificate of non-copositivity entirely. This suggests that the discretization scheme should be well-tailored to the problem at hand; Appendix 6.2 provides guidance for choosing a discretization size based on the coefficients of the Ising Hamiltonian.

**Multiple cuts** Following standard convention, this work assumes that the copositivity oracle returns a single value. In contrast, in practice, many of the aforementioned Ising solvers involve multiple readouts. Each of these solutions can be used to construct a cut, where negative, zero, and positive Ising objective values correspond to deep, neutral, and shallow cuts, respectively. Adding multiple cuts during each iteration is an effective heuristic for improving the convergence rate of the cutting-plane algorithm. While the true ground state corresponds to the deepest cut, the convergence rate guarantees stated in Table 1 hold so long as a neutral or deep cut is added at each iteration. Consequently, the proposed approach is not overly reliant on the Ising solver’s ability to identify the ground state and is resilient to heuristics. Critically, this raises the question of how to proceed if the Ising solver fails to return a certificate of non-copositivity, which will likely depend on problem specifics, such as the current outer approximation, the objective values of the samples, and the solver itself. For example, if the Ising solver returns positive but small solutions, depending on the current outer approximation, the addition of shallow cuts can still reduce the search space. On the other hand, if all non-zero solutions result in a large objective value, one could increase confidence that the test point is feasible by increasing the number of discretization points and readouts.

## 4 Experiments

We conducted an investigation of the proposed method on the maximum clique problem, which finds the largest complete subgraph of a graph. Given a graph, the maximum clique problem can be formulated as a completely positive program

$$\begin{aligned} & \text{maximize} && \langle \mathbf{1}\mathbf{1}^\top, X \rangle \\ & X \in \mathbb{R}^{n \times n} \\ & \text{subject to} && \langle \bar{A} + I, X \rangle = 1, \\ & && X \in \mathcal{C}_n^*, \end{aligned} \tag{19}$$

where  $\bar{A}$  is the adjacency matrix of the graph’s complement [58]. The dual of (19) is the following copositive program:

$$\begin{aligned} & \text{minimize} && \lambda \\ & \lambda \in \mathbb{R} \\ & \text{subject to} && \lambda(I + \bar{A}) - \mathbf{1}\mathbf{1}^\top \in \mathcal{C}_n. \end{aligned} \tag{20}$$

This copositive program only has one variable regardless of the graph’s number of vertices or edges. However, the copositivity check’s size is determined by the number of vertices,  $n$ , which impacts the complexity of computing the cuts from the certificates of non-copositivity. The number of edges can be used to upper-bound the size of the maximum clique, thus determining the size of the initial feasible region; however, its effect on the complexity of checking copositivity is unclear.

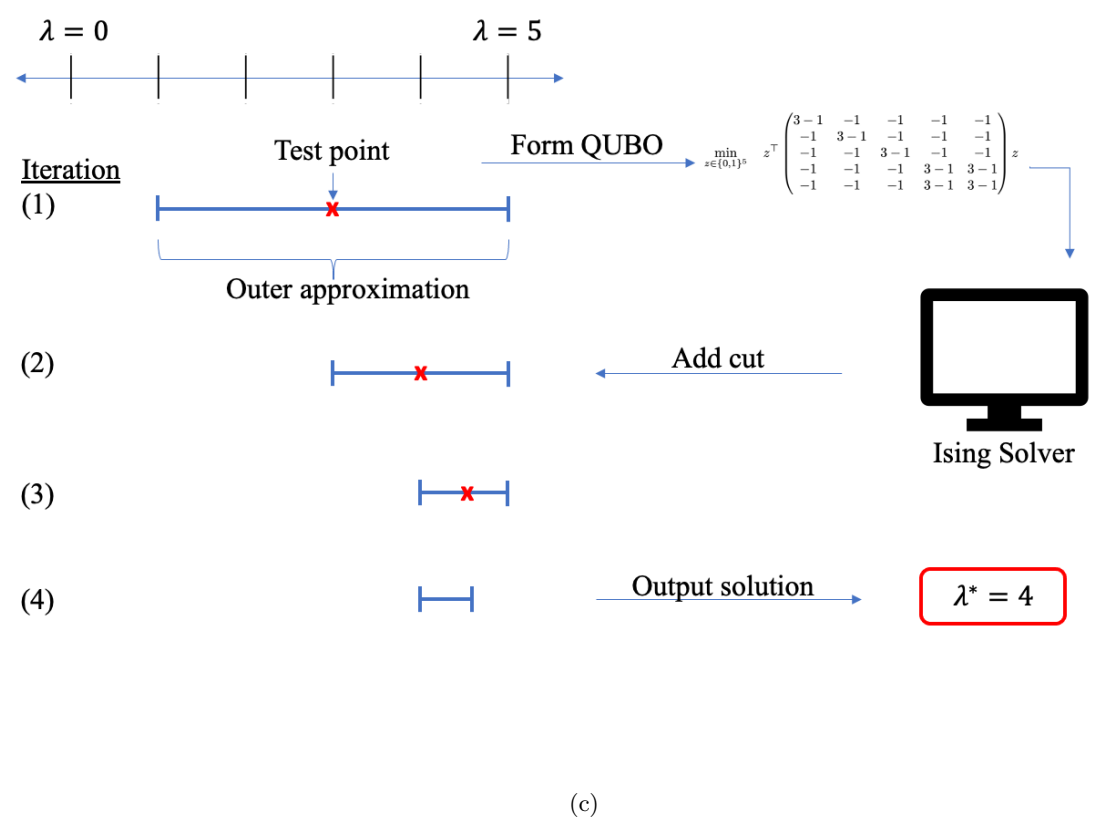
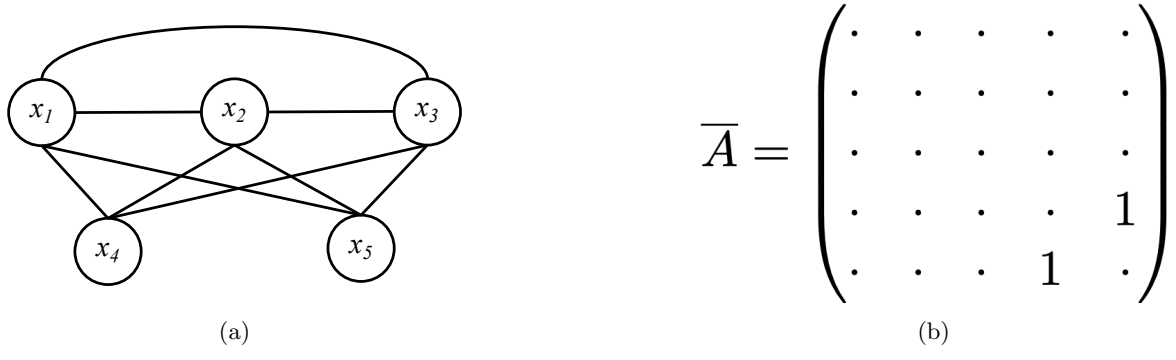


Figure 2: Figure 2a depicts a small maximum clique example where there are edges between all vertices except  $x_4$  and  $x_5$ . Figure 2b depicts the adjacency matrix of graph 2a's complement, which has a single edge between vertices  $x_4$  and  $x_5$ . Figure 2c depicts the solution process for the copositive cutting-plane algorithm.

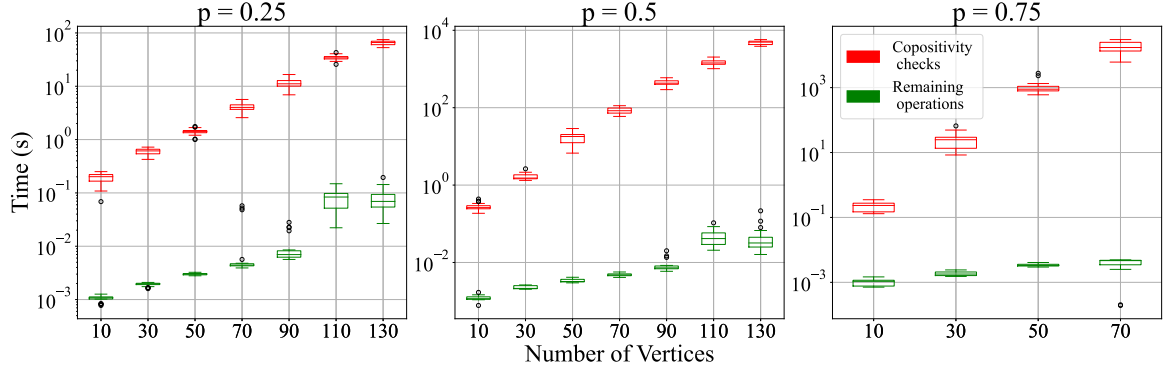


Figure 3: This figure plots the time spent on the copositivity checks versus all other operations in the proposed method. The copositivity checks grow exponentially with the number of vertices, while the other operations grow modestly.

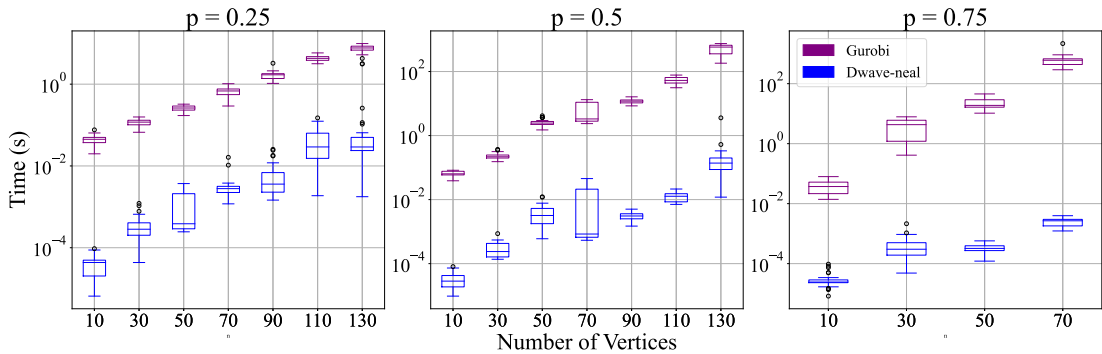


Figure 4: This figure plots the time to target to 99% confidence of the Simulated Annealing (SA) implementation in `dwave-neal` against the solution time of `Gurobi` for two discretization points in the copositivity checks. We solved each copositivity check with 100 sweeps and 1000 reads. For all densities, both methods scale exponentially with the number of vertices in the graph; however, SA is several orders of magnitude faster than `Gurobi`.

To study the scaling of the proposed approach, we considered random max-clique problems with  $10, 30, \dots, 130$  vertices. For each graph size, we generated 25 random Erdős-Renyi instances with edge densities  $p \in \{0.25, 0.5, 0.75\}$  and solved to global optimality using the proposed copositive cutting plane algorithm. The copositivity checks were conducted by solving Anstreicher’s MILP characterization of copositivity [53], using `Gurobi` version 9.0.3 [59]. All experiments were run on an AMD Ryzen 7 1800X Eight-Core Processor@3.6GHz with 64GB of RAM restricted to a single thread.

We first evaluated whether the copositive cutting-plane algorithm shifts the complexity of the solution process onto the copositivity checks by profiling each component of the algorithm separately. Figure 3 plots the time the copositive cutting plane algorithm spent on the copositivity checks versus other operations (updating the outer approximation and computing test points). The time spent on the copositivity checks scales exponentially with the number of vertices in the graph, while the time spent on other operations grows modestly. This is because Problem (19) only has one constraint regardless of the graph’s number of vertices or edges. In contrast, the size of the copositivity check is exactly equal to the number of vertices in the graph. Both the theoretical analysis and empirical results confirm that the proposed approach shifts the complexity of the copositive program onto the copositivity checks. This experiment shows that the proposed methodology is particularly effective for problems whose constraints remain constant or grow modestly with problem size.

To investigate potential speedups from using a stochastic Ising solver, we re-solved each copositivity check that yielded a certificate of non-copositivity using Simulated Annealing (SA) through the software `dwave-neal` version 0.5.9, a SA sampler [60], i.e., a solver that returns samples on the solutions distribution generated by SA. Because SA is not guaranteed to find the global optima in a single annealing cycle, we define a probabilistic notion of time to target. In particular, we follow [61]

and define the time to target with  $s$  confidence to be the number of repetitions to find the ground state at least once with probability  $s$  multiplied by the time for each annealing cycle,  $T_{\text{anneal}}$ , i.e.,

$$\text{TTT}_s = T_{\text{anneal}} \frac{\log(1-s)}{\log(1-\hat{p}_{\text{succ}})}, \quad (21)$$

where  $\hat{p}_{\text{succ}}$  is the expected value of the returned solution divided by the ground state/minimum. This results in a probability of success that interpolates between counting only ground state solutions and counting all certificates of non-copositivity as successes by considering the relative quality of each sample. We will also consider analogous scenarios where only ground state solutions are counted as success; we reserve the terminology ‘‘time to solution’’,  $\text{TTS}_s = T_{\text{anneal}} \frac{\log(1-s)}{\log(1-p_{\text{succ}})}$ , for such cases to distinguish from the previously defined time to target. The values of  $\hat{p}_{\text{succ}}$  and  $p_{\text{succ}}$  is evaluated empirically over 1000 samples/reads. The time per annealing cycle,  $T_{\text{anneal}}$ , was evaluated as the total wall-clock time (for all reads) divided by the number of reads. All other **dwave-neal** parameters were left as their default values.

For each copositivity check solved, we considered discretizations corresponding to  $\min_{z \in \{0,1\}^n} \hat{z}^\top M \hat{z}$ . We solved each copositivity check with 100 sweeps and 1000 reads<sup>2</sup>. Figure 4 plots the time to target with 99% confidence from SA against the solution time from **Gurobi**<sup>3</sup>. We see that for all discretization sizes, **dwave-neal** can consistently find certificates of non-copositivity in orders of magnitude less time than **Gurobi**. Notably, SA and **Gurobi** demonstrate similar scaling with respect to the number of vertices.

Unlike SA, which operates without reference to rigorous optimality bounds, **Gurobi**’s solution process tracks both upper and lower bounds on the objective value and terminates only when they reach user-specified stopping conditions. To evaluate whether the optimal objective is found early in the solution process and time is spent closing the upper bounds, we plotted **Gurobi**’s lower and upper bounds progress against time together with  $\text{TTT}_{0.99}$  and  $\text{TTT}_{0.999}$  in Figure 5 for instances with density  $p = 0.25$ . Analogous plots for other densities are included in the Appendix. For each graph size, we plotted the instances where the ratio between **Gurobi**’s solution time and  $\text{TTT}_{0.99}$  is the greatest (top row) and least (bottom row)—all instances were run with 100 sweeps. For each instance, we plot **Gurobi**’s upper bound (blue) and best objective found (orange), and **dwave-neal**  $\text{TTT}_{0.99}$  (green), and  $\text{TTT}_{0.999}$  (purple). We found that in most instances, **dwave-neal** reaches the time to target with 99.9% confidence before **Gurobi** even returns a callback (i.e., when the purple line does not intersect either of the blue or orange lines); this is likely due to an initial pre-processing step. We only found one instance where **Gurobi** was able to confirm optimality at the first callback (Figure 11)—even so,  $\text{TTT}_{0.999}$  is nearly two orders of magnitude faster than **Gurobi**’s solution time in this instance.

Next, we compared the copositive cutting-plane algorithm with the SA implementation in **dwave-neal** as the Ising solver against solving a MIP formulation of maximum-clique directly with **Gurobi**. For the copositive cutting-plane algorithm, each copositivity check was conducted with 250 reads and 100 sweeps. Because **dwave-neal** may fail to find a certificate for some non-copositive matrices, this method may incorrectly reduce the upper bound in the outer approximation; however, cannot incorrectly update the lower bound. Consequently, the solution returned was determined by rounding the lower bound up to the nearest integer. We found that out of all trials, only four instances returned a solution less than the true optimum (two each for graphs of 110 and 130 nodes and edge density  $p = 0.75$ ). All of these instances were solved to global optimality by increasing the number of reads to 400. **Gurobi**’s solution time was evaluated on the following MIP formulation of maximum clique:

$$\begin{aligned} & \underset{x \in \{0,1\}^n}{\text{minimize}} && \mathbf{1}^\top x \\ & \text{subject to} && x_i x_j = 0, \quad \forall (i,j) \in \overline{E}, \end{aligned} \quad (22)$$

where  $\overline{E}$  is the edges in the complement graph<sup>4</sup>. This is a MIP with  $n$  binary variables, where  $n$  is the number of vertices in the graph, and  $|\overline{E}|$  constraints (i.e., the number of edges in the complement

<sup>2</sup>While the performance of **dwave-neal** depends on the number of sweeps, we found that optimizing the number of sweeps does not result in significant reductions in the time to target. We provide further discussion in the Appendix 6.3.

<sup>3</sup>Note that **Gurobi**’s solution time in Figure 4 is different from copositivity checks profiling in Figure 3. This is because only non-copositive instances were considered for this comparison, while all instances, including copositive ones, were included in the profiling comparison.

<sup>4</sup>We also considered a formulation with additive constraints, i.e.  $x_i + x_j \leq 1, \forall (i,j) \in \overline{E}$ , but did not see significant differences in performance compared to the multiplicative constraints.

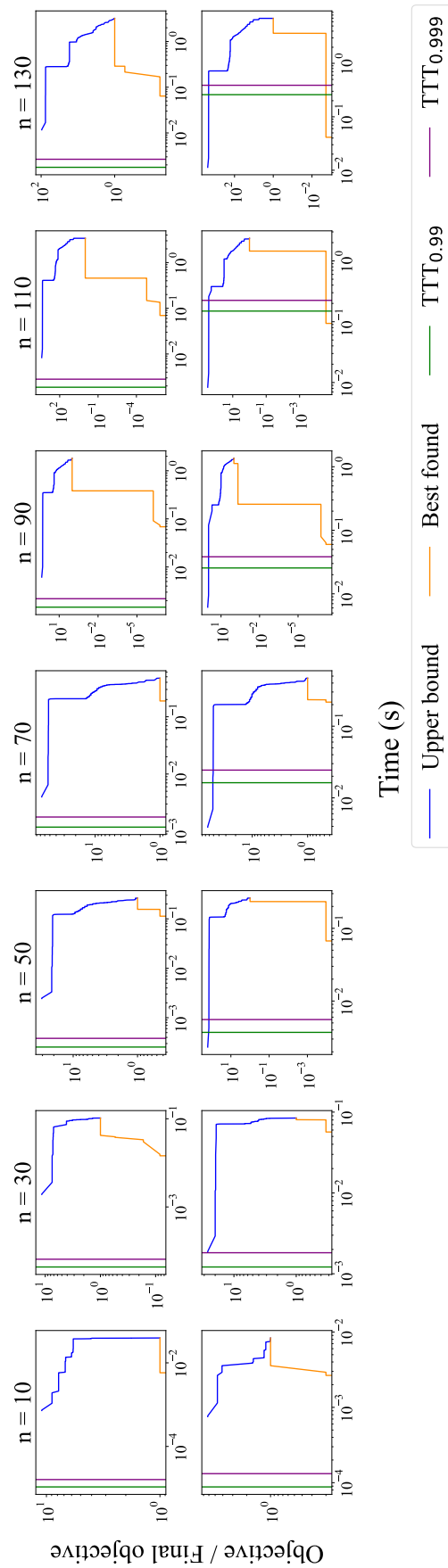


Figure 5: This figure depicts sample trajectories of Gurobi's upper and lower bounds against  $TTT_{0.99}$  and  $TTT_{0.999}$  for edge density  $p = 0.25$ . For each graph size, the top row represents the instance where the ratio between Gurobi's solution time and  $TTT_{0.99}$  is the greatest, and the bottom row represents the instance where the ratio is the smallest—all instances were run with 100 sweeps. In most instances, **dwave-neal** reaches the  $TTT_{0.999}$  confidence before Gurobi even returns a callback (i.e., when the purple line does not intersect either of the blue or orange lines).



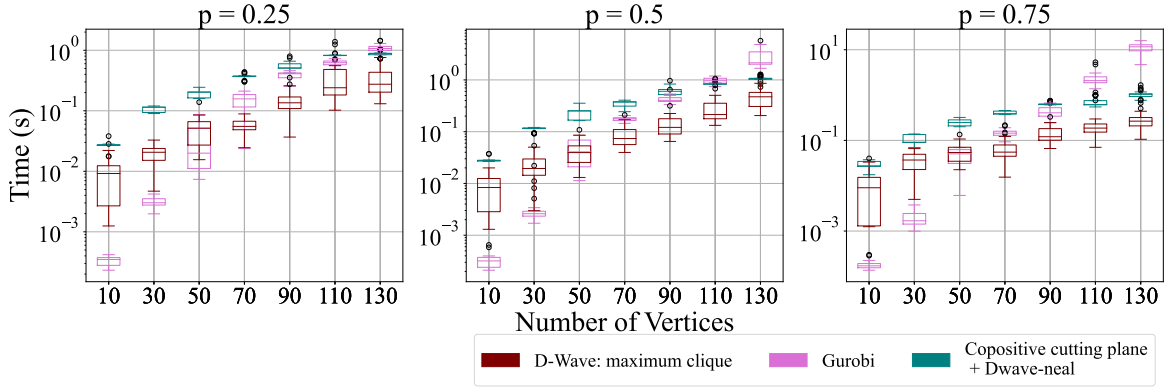


Figure 6: This figure plots the solution time for the copositive cutting-plane algorithm with the Simulated Annealing implementation in `dwave-neal` as the Ising solver, the solution time when solving a mixed-integer programming (MIP) formulation of maximum-clique directly with `Gurobi`, and the corresponding  $\text{TTT}_{0.999}$  from D-Wave Ocean `maximum_clique` for penalty weight 1. While `Gurobi`'s solution time is orders of magnitude faster than the copositive cutting-plane algorithm for the smallest graph sizes, the copositive cutting-plane algorithm exhibits better scaling than `Gurobi` and outperforms it for larger graph sizes. `maximum_clique` exhibits a similar scaling to the copositive cutting-plane algorithm but is half an order of magnitude faster.

graph). Figure 6 plots the solution time for the `Gurobi` MIP formulation against that of the copositive cutting-plane algorithm. We find that for smaller graph sizes, `Gurobi`'s solution time is orders of magnitude faster than the copositive cutting-plane algorithm. However, the copositive cutting-plane algorithm exhibits better scaling with respect to the number of nodes than `Gurobi`, and outperforms it for larger graph sizes.

Finally, we investigated the effectiveness of directly converting the maximum clique problem to an Ising problem using a standard penalty formulation. To do so, we solved each of the maximum clique problem instances using the D-Wave Ocean `maximum_clique` solver<sup>5</sup> with `dwave-neal` as the sampler and a range of penalty weights in  $\{2^{-1}, 2^0, \dots, 2^4\}$ ; the number of sweeps were left to their default value of 1000. This results in a QUBO with  $n$  variables and  $|\overline{E}|$  quadratic terms. For each instance, we conducted 1000 reads and evaluated the average normalized sample size (the size of the returned solution divided by the ground truth maximum clique size) and the fraction of reads that resulted in a valid clique; a ground state solution is one that is both a valid clique and has a normalized sample size of 1. We computed the probability of success,  $p_{\text{succ}}$ , as the fraction of reads that resulted in a ground state solution, which was subsequently used to derive the time to solution to 99.9% confidence. Figure 7 plots each of these metrics as a function of the penalty weights and graph size for edge density  $p = 0.25$ . Analogous plots for other densities are included in the Appendix. For penalty weights 0.5 and 1, the normalized sample size is often greater than 1, resulting in samples that do not represent a valid clique. For penalty weights 2, 4, 8, and 16, most samples were valid cliques; however, the normalized sample sizes were typically less than 1—these represent non-maximum cliques. Generally, as the penalty weight is increased, the normalized sample size decreases, and the fraction of valid cliques increases. This aligns with the interpretation that the penalty weight represents a trade-off between satisfying the constraints versus optimizing the objective. These empirical results also corroborate the analytical results of [62], which state that the minimum valid penalty weight for the stable set of a graph is 1. Given that `maximum_clique` represents the maximum clique problem as finding the stable set of the graph built with the complement of the original edges, the bound on the penalty weight is valid. This experiment demonstrates that while the penalty formulation may be an effective heuristic, it typically requires carefully tuning the penalty weights to optimize the trade-off between satisfying the constraints and optimizing the objective.

Figure 6 plots the corresponding  $\text{TTT}_{0.999}$  from D-Wave Ocean `maximum_clique` for penalty weight 1 against the `Gurobi` solution time and the copositive cutting-plane solution time. We observe that `maximum_clique` exhibits a similar scaling to the copositive cutting-plane algorithm—likely because they both use `dwave-neal` as a sampler—but is half an order of magnitude faster. This is an un-

<sup>5</sup>[https://docs.ocean.dwavesys.com/projects/dwave-networkx/en/latest/reference/algorithms/generated/dwave\\_networkx.maximum\\_clique.html](https://docs.ocean.dwavesys.com/projects/dwave-networkx/en/latest/reference/algorithms/generated/dwave_networkx.maximum_clique.html)

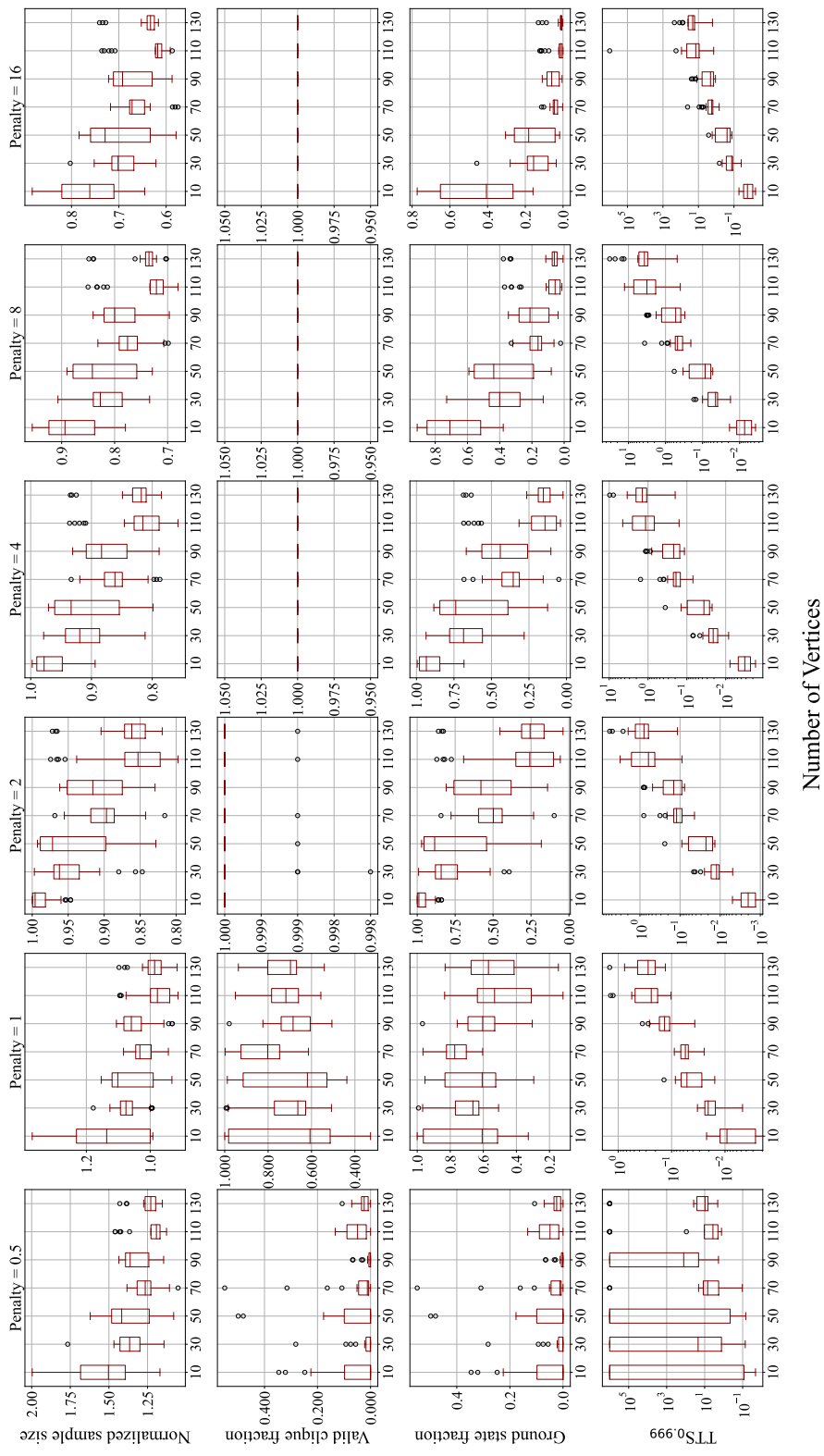


Figure 7: This figure plots the normalized sample size (the size of the returned solution divided by the ground truth maximum clique size) and the fraction of reads that resulted in a valid clique for graph density  $p = 0.25$ . These figures were used to compute the fraction of reads resulting in a ground state solution and the corresponding  $\text{TTS}_{0.999}$  (also plotted). As the penalty weight is increased, the normalized sample size decreases, and the fraction of valid cliques increases. This highlights the delicate trade-off between constraints and the objective in penalty formulations.

surprising observation given that `maximum_clique` is a heuristic that operates without reference to optimality bounds. In contrast, both Gurobi and the copositivity cutting-plane algorithm are complete methods. Indeed the choice of 0.999 for the confidence of TTS is arbitrary, as heuristic solvers are not easily compared to complete solvers. These results suggest that the copositive cutting-plane method inherits its favorable scaling from the heuristic Ising solver while maintaining the optimality guarantees of a convergent algorithm.

## 5 Conclusions

In this paper, we have proposed a framework for solving mixed-binary quadratic programming problems with optimality guarantees using a heuristic and black-box Ising solver. Our framework relies on Burer’s convex reformulation of such problems using completely positive programming—our first contribution is to extend this result and show that under mild conditions, the dual copositive program exhibits strong duality. We then propose a hybrid quantum-classic solution algorithm based on cutting-plane algorithms, where an Ising solver is used to construct the separation oracle. Critically, the run-time of the components handled by the classical computer scales polynomially with the number of constraints in the original mixed-binary quadratic program. This suggests that if our approach is applied to a problem with exponential scaling, the complexity is shifted on the subroutine carried out by the hardware accelerator, e.g., the quantum computer. Our proposed approach is particularly appealing because it suggests that the proposed approach could take advantage of any speedup that exists even without an explicit characterization of what that speedup is.

While the proposed framework seems like a promising way forward for utilizing quantum/quantum-inspired Ising solvers, several crucial questions remain open. This first question is how the algorithm should proceed if the Ising solver fails to find a certificate of non-copositivity. Could one use a classical computer to locally refine approximate primal-dual optimal solutions? The second question is the issue of discretizing the copositivity checks. As an alternative to a uniform discretization, are there ways to locally refine or systematically construct heterogeneous discretizations that better pinpoint a certificate of non-copositivity? Alternatively, could one reparametrize the copositivity check so that the certificates of non-copositivity are better aligned with the discretization points in a coarser grid? We hope that this paper is the first step in answering these questions and serves as an inspiration to the community to embrace Ising solvers with convergent mathematical programming algorithms.

## Acknowledgements

This work was supported by NSF CCF (grant #1918549), NASA Academic Mission Services (contract NNA16BD14C – funded under SAA2-403506). R.B. acknowledges support from the NASA/USRA Feynman Quantum Academy Internship program. The authors wish to thank Aaron Lott, Luis Zuluaga, and Juan Vera for helpful input and discussions during the development of these ideas.

## References

- [1] M. W. Johnson, M. H. Amin, S. Gildert, T. Lanting, F. Hamze, N. Dickson, R. Harris, A. J. Berkley, J. Johansson, P. Bunyk *et al.*, “Quantum annealing with manufactured spins,” *Nature*, vol. 473, no. 7346, pp. 194–198, 2011.
- [2] E. Farhi, J. Goldstone, and S. Gutmann, “A quantum approximate optimization algorithm,” *arXiv preprint arXiv:1411.4028*, 2014.
- [3] T. Honjo, T. Sonobe, K. Inaba, T. Inagaki, T. Ikuta, Y. Yamada, T. Kazama, K. Enbutsu, T. Umeki, R. Kasahara *et al.*, “100,000-spin coherent Ising machine,” *Science advances*, vol. 7, no. 40, p. eabh0952, 2021.
- [4] C. Gambella and A. Simonetto, “Multiblock ADMM heuristics for mixed-binary optimization on classical and quantum computers,” *IEEE Transactions on Quantum Engineering*, vol. 1, pp. 1–22, 2020.
- [5] C.-Y. Chang, E. Jones, Y. Yao, P. Graf, and R. Jain, “On Hybrid Quantum and Classical Computing Algorithms for Mixed-Integer Programming,” *arXiv e-prints*, pp. arXiv–2010, 2020.

- [6] Z. Zhao, L. Fan, and Z. Han, “Hybrid Quantum Benders’ Decomposition For Mixed-integer Linear Programming,” *arXiv preprint arXiv:2112.07109*, 2021.
- [7] N. G. Paterakis, “Hybrid Quantum-Classical Multi-cut Benders Approach with a Power System Application,” *arXiv preprint arXiv:2112.05643*, 2021.
- [8] S. Burer, “On the copositive representation of binary and continuous nonconvex quadratic programs,” vol. 120, no. 2, p. 479–495, 2009.
- [9] A. Yurtsever, T. Birdal, and V. Golyanik, “Q-FW: A Hybrid Classical-Quantum Frank-Wolfe for Quadratic Binary Optimization,” *arXiv preprint arXiv:2203.12633*, 2022.
- [10] D. Venturelli, D. Marchand, and G. Rojo, “Job shop scheduling solver based on quantum annealing,” in *Proc. of ICAPS-16 Workshop on Constraint Satisfaction Techniques for Planning and Scheduling (COPLAS)*, 2016, pp. 25–34.
- [11] S. Harwood, C. Gambella, D. Trenev, A. Simonetto, D. Bernal, and D. Greenberg, “Formulating and solving routing problems on quantum computers,” *IEEE Transactions on Quantum Engineering*, vol. 2, pp. 1–17, 2021.
- [12] C. F. Negre, H. Ushijima-Mwesigwa, and S. M. Mniszewski, “Detecting multiple communities using quantum annealing on the D-Wave system,” *Plos one*, vol. 15, no. 2, p. e0227538, 2020.
- [13] A. Lucas, “Ising formulations of many NP problems,” *Frontiers in physics*, p. 5, 2014.
- [14] R. A. Brown, E. Schmerling, N. Azizan, and M. Pavone, “A Unified View of SDP-based Neural Network Verification through Completely Positive Programming,” in *International Conference on Artificial Intelligence and Statistics*. Pmlr, 2022, pp. 9334–9355.
- [15] C. A. Floudas and C. E. Gounaris, “A review of recent advances in global optimization,” *Journal of Global Optimization*, vol. 45, no. 1, pp. 3–38, 2009.
- [16] S. Boyd, N. Parikh, E. Chu, B. Peleato, J. Eckstein *et al.*, “Distributed optimization and statistical learning via the alternating direction method of multipliers,” *Foundations and Trends<sup>®</sup> in Machine learning*, vol. 3, no. 1, pp. 1–122, 2011.
- [17] S. Diamond, R. Takapoui, and S. Boyd, “A general system for heuristic minimization of convex functions over non-convex sets,” *Optimization Methods and Software*, vol. 33, no. 1, pp. 165–193, 2018.
- [18] Y. Wang, W. Yin, and J. Zeng, “Global convergence of ADMM in nonconvex nonsmooth optimization,” *Journal of Scientific Computing*, vol. 78, no. 1, pp. 29–63, 2019.
- [19] H. Attouch, J. Bolte, and B. F. Svaiter, “Convergence of descent methods for semi-algebraic and tame problems: proximal algorithms, forward–backward splitting, and regularized Gauss–Seidel methods,” *Mathematical Programming*, vol. 137, no. 1, pp. 91–129, 2013.
- [20] M. Booth, S. Reinhardt, and A. Roy, “Partitioning Optimization Problems for Hybrid Classical/Quantum Execution,” D-Wave, Tech. Rep., 2017.
- [21] F. Glover and S. Hanafi, “Tabu search and finite convergence,” *Discrete Applied Mathematics*, vol. 119, no. 1-2, pp. 3–36, 2002.
- [22] H. Alghassi, R. Dridi, and S. Tayur, “Graver bases via quantum annealing with application to non-linear integer programs,” *arXiv preprint arXiv:1902.04215*, 2019.
- [23] T. Albash and D. A. Lidar, “Adiabatic quantum computation,” *Reviews of Modern Physics*, vol. 90, no. 1, p. 015002, 2018.
- [24] P. Hauke, H. G. Katzgraber, W. Lechner, H. Nishimori, and W. D. Oliver, “Perspectives of quantum annealing: Methods and implementations,” *Reports on Progress in Physics*, vol. 83, no. 5, p. 054401, 2020.
- [25] M. Cerezo, A. Arrasmith, R. Babbush, S. C. Benjamin, S. Endo, K. Fujii, J. R. McClean, K. Mitarai, X. Yuan, L. Cincio *et al.*, “Variational quantum algorithms,” *Nature Reviews Physics*, vol. 3, no. 9, pp. 625–644, 2021.

- [26] E. Farhi and A. W. Harrow, “Quantum supremacy through the quantum approximate optimization algorithm,” *arXiv preprint arXiv:1602.07674*, 2016.
- [27] J. Preskill, “Quantum computing in the nisc era and beyond,” *Quantum*, vol. 2, p. 79, 2018.
- [28] A. Uvarov and J. D. Biamonte, “On barren plateaus and cost function locality in variational quantum algorithms,” *Journal of Physics A: Mathematical and Theoretical*, vol. 54, no. 24, p. 245301, 2021.
- [29] M. Willsch, D. Willsch, F. Jin, H. De Raedt, and K. Michielsen, “Benchmarking the quantum approximate optimization algorithm,” *Quantum Information Processing*, vol. 19, no. 7, pp. 1–24, 2020.
- [30] M. P. Harrigan, K. J. Sung, M. Neeley, K. J. Satzinger, F. Arute, K. Arya, J. Atalaya, J. C. Bardin, R. Barends, S. Boixo *et al.*, “Quantum approximate optimization of non-planar graph problems on a planar superconducting processor,” *Nature Physics*, vol. 17, no. 3, pp. 332–336, 2021.
- [31] Y. R. Sanders, D. W. Berry, P. C. Costa, L. W. Tessler, N. Wiebe, C. Gidney, H. Neven, and R. Babbush, “Compilation of fault-tolerant quantum heuristics for combinatorial optimization,” *PRX Quantum*, vol. 1, no. 2, p. 020312, 2020.
- [32] Y. Yamamoto, K. Aihara, T. Leleu, K.-i. Kawarabayashi, S. Kako, M. Fejer, K. Inoue, and H. Takesue, “Coherent Ising machines—Optical neural networks operating at the quantum limit,” *npj Quantum Information*, vol. 3, no. 1, pp. 1–15, 2017.
- [33] N. Mohseni, P. L. McMahon, and T. Byrnes, “Ising machines as hardware solvers of combinatorial optimization problems,” *Nature Reviews Physics*, pp. 1–17, 2022.
- [34] S. Boyd and L. Vandenberghe, “Convex Optimization,” 2004.
- [35] D. Bertsekas, *Convex optimization theory*. Athena Scientific, 2009, vol. 1.
- [36] K. G. Murty and S. N. Kabadi, “Some NP-complete problems in quadratic and nonlinear programming,” *Mathematical Programming*, vol. 39, no. 2, pp. 117–129, 1987.
- [37] P. A. Parrilo, “Structured Semidefinite Programs and Semialgebraic Geometry Methods in Robustness and Optimization,” Ph.D. dissertation, 2000.
- [38] J. B. Lasserre, “Global optimization with polynomials and the problem of moments,” *SIAM Journal on optimization*, vol. 11, no. 3, pp. 796–817, 2001.
- [39] M. Dür and F. Rendl, “Conic optimization: a survey with special focus on copositive optimization and binary quadratic problems,” *EURO Journal on Computational Optimization*, vol. 9, p. 100021, 2021.
- [40] S. Burer, “Copositive programming,” in *Handbook on semidefinite, conic and polynomial optimization*. Springer, 2012, pp. 201–218.
- [41] M. Dür, “Copositive programming—a survey,” in *Recent advances in optimization and its applications in engineering*. Springer, 2010, pp. 3–20.
- [42] L. A. Rademacher, “Approximating the centroid is hard,” in *Proceedings of the twenty-third annual symposium on Computational geometry*, 2007, pp. 302–305.
- [43] A. Y. Levin, “An algorithm for minimizing convex functions,” in *Doklady Akademii Nauk*, vol. 160, no. 6. Russian Academy of Sciences, 1965, pp. 1244–1247.
- [44] N. Z. Shor, “Cut-off method with space extension in convex programming problems,” *Cybernetics*, vol. 13, no. 1, pp. 94–96, 1977.
- [45] D. B. Yudin and A. S. Nemirovski, “Evaluation of the information complexity of mathematical programming problems,” *Ekonomika i Matematicheskie Metody*, vol. 12, pp. 128–142, 1976.
- [46] L. G. Khachiyan, “Polynomial algorithms in linear programming,” *USSR Computational Mathematics and Mathematical Physics*, vol. 20, no. 1, pp. 53–72, 1980.

- [47] L. G. Khachiyan, S. P. Tarasov, and I. Erlikh, “The method of inscribed ellipsoids,” in *Soviet Math. Dokl*, vol. 37, no. 1, 1988, pp. 226–230.
- [48] Y. Nesterov and A. Nemirovski, “Self-concordant functions and polynomial time methods in convex programming,” *USSR Academy of Sciences, Central Economic&Mathematical Institute, Moscow*, 1989.
- [49] P. M. Vaidya, “A new algorithm for minimizing convex functions over convex sets,” in *30th Annual Symposium on Foundations of Computer Science*. IEEE Computer Society, 1989, pp. 338–343.
- [50] D. S. Atkinson and P. M. Vaidya, “A cutting plane algorithm for convex programming that uses analytic centers,” *Mathematical Programming*, vol. 69, no. 1, pp. 1–43, 1995.
- [51] D. Bertsimas and S. Vempala, “Solving convex programs by random walks,” *Journal of the ACM (JACM)*, vol. 51, no. 4, pp. 540–556, 2004.
- [52] Y. T. Lee, A. Sidford, and S. C.-w. Wong, “A faster cutting plane method and its implications for combinatorial and convex optimization,” in *2015 IEEE 56th Annual Symposium on Foundations of Computer Science*. Ieee, 2015, pp. 1049–1065.
- [53] K. M. Anstreicher, “Testing copositivity via mixed-integer linear programming,” *Linear Algebra and its Applications*, vol. 609, pp. 218–230, 2021.
- [54] M. Dür and J.-B. Hiriart-Urruty, “Testing copositivity with the help of difference-of-convex optimization,” *Mathematical Programming*, vol. 140, no. 1, pp. 31–43, 2013.
- [55] J.-B. Hiriart-Urruty and A. Seeger, “A variational approach to copositive matrices,” *SIAM review*, vol. 52, no. 4, pp. 593–629, 2010.
- [56] C. Brás, G. Eichfelder, and J. Júdice, “Copositivity tests based on the linear complementarity problem,” *Computational Optimization and Applications*, vol. 63, no. 2, pp. 461–493, 2016.
- [57] W. Xia, J. C. Vera, and L. F. Zuluaga, “Globally solving nonconvex quadratic programs via linear integer programming techniques,” *INFORMS Journal on Computing*, vol. 32, no. 1, pp. 40–56, 2020.
- [58] E. De Klerk and D. V. Pasechnik, “Approximation of the stability number of a graph via copositive programming,” *SIAM Journal on Optimization*, vol. 12, no. 4, pp. 875–892, 2002.
- [59] *Gurobi Optimizer Reference Manual*, 2022, available at <http://www.gurobi.com>.
- [60] *dwave-neal Documentation*, D-Wave Systems Inc, 2021, available at <https://docs.ocean.dwavesys.com/-/downloads/neal/en/latest/pdf/>.
- [61] T. F. Rønnow, Z. Wang, J. Job, S. Boixo, S. V. Isakov, D. Wecker, J. M. Martinis, D. A. Lidar, and M. Troyer, “Defining and detecting quantum speedup,” *science*, vol. 345, no. 6195, pp. 420–424, 2014.
- [62] R. Quintero, D. Bernal, T. Terlaky, and L. F. Zuluaga, “Characterization of QUBO reformulations for the maximum k-colorable subgraph problem,” *Quantum Information Processing*, vol. 21, no. 3, pp. 1–36, 2022.
- [63] S. Kim and M. Kojima, “Strong duality of a conic optimization problem with two cones and a single equality constraint,” *arXiv preprint arXiv:2111.03251*, 2021.
- [64] S. Karimi and P. Ronagh, “Practical integer-to-binary mapping for quantum annealers,” *Quantum Information Processing*, vol. 18, no. 4, pp. 1–24, 2019.
- [65] J. Bergstra, D. Yamins, and D. Cox, “Making a science of model search: Hyperparameter optimization in hundreds of dimensions for vision architectures,” in *International conference on machine learning*. Pmlr, 2013, pp. 115–123.

## 6 Appendix

### 6.1 Proof of strong duality

Problem (CPP) is equivalent to the following homogenous form completely positive program (i.e.,  $\min(\text{CPP}) = \min(\text{Hom-CPP})$ ):

$$\begin{aligned} & \underset{x \in \mathbb{R}^n, X \in \mathbb{R}^{n \times n}}{\text{minimize}} && \left\langle \begin{pmatrix} Q & c \\ c^\top & \cdot \end{pmatrix}, \begin{pmatrix} X & x \\ x^\top & 1 \end{pmatrix} \right\rangle \\ & \text{subject to} && \left\langle \begin{pmatrix} A_{i,*}^\top A_{i,*} & -b_i A_{i,*}^\top \\ -b_i A_{i,*} & b_i^2 \end{pmatrix}, \begin{pmatrix} X & x \\ x^\top & 1 \end{pmatrix} \right\rangle = 0, \\ & && \left\langle \begin{pmatrix} -\mathbf{1}_{\{j\}} \mathbf{1}_{\{j\}}^\top & \frac{1}{2} \mathbf{1}_{\{j\}} \\ \frac{1}{2} \mathbf{1}_{\{j\}}^\top & \cdot \end{pmatrix}, \begin{pmatrix} X & x \\ x^\top & 1 \end{pmatrix} \right\rangle = 0, \forall j \in B, \\ & && \begin{pmatrix} X & x \\ x^\top & 1 \end{pmatrix} \in \mathcal{C}_{n+1}^*. \end{aligned} \tag{Hom-CPP}$$

This form will be useful for proving strong duality. Because the homogenized form of the equality constraints form a cone, this perspective will help prove strong duality between Problem (CPP) and its dual. The Lagrangian dual of (Hom-CPP) is the following copositive optimization problem:

$$\begin{aligned} & \underset{\mu, \lambda, \gamma}{\text{maximize}} && \gamma \\ & \text{subject to} && \hat{M}(\mu, \lambda, \gamma) \in \mathcal{C}_{n+1}, \end{aligned} \tag{Hom-COP}$$

where  $\hat{M}(\mu, \lambda, \gamma)$  is defined as

$$\begin{aligned} \hat{M}(\mu, \lambda, \gamma) & := \begin{pmatrix} Q & c \\ c^\top & \cdot \end{pmatrix} - \sum_i \mu_i \begin{pmatrix} A_{i,*}^\top A_{i,*} & -b_i A_{i,*}^\top \\ -b_i A_{i,*} & b_i^2 \end{pmatrix} \\ & - \sum_{j \in B} \lambda_j \begin{pmatrix} -\mathbf{1}_{\{j\}} \mathbf{1}_{\{j\}}^\top & \frac{1}{2} \mathbf{1}_{\{j\}} \\ \frac{1}{2} \mathbf{1}_{\{j\}}^\top & \cdot \end{pmatrix} - \gamma \begin{pmatrix} \cdot & \cdot \\ \cdot & 1 \end{pmatrix}. \end{aligned} \tag{23}$$

**Theorem 6.1** (Homogeneous Strong Duality). *If Problem (MBQP) is feasible with bounded feasible region, then strong duality holds between Problems (Hom-CPP) and (Hom-COP).*

*Proof.* Notice that the set of affine constraints,

$$\mathcal{NULC} := \left\{ \tilde{X} \mid \left\langle \begin{pmatrix} A_{i,*}^\top A_{i,*} & -b_i A_{i,*}^\top \\ -b_i A_{i,*} & b_i^2 \end{pmatrix}, \tilde{X} \right\rangle = 0, \left\langle \begin{pmatrix} -\mathbf{1}_{\{j\}} \mathbf{1}_{\{j\}}^\top & \frac{1}{2} \mathbf{1}_{\{j\}} \\ \frac{1}{2} \mathbf{1}_{\{j\}}^\top & \cdot \end{pmatrix}, \tilde{X} \right\rangle = 0 \right\}, \tag{24}$$

forms a cone. So, we could express (Hom-CPP) as the following optimization problem:

$$\begin{aligned} & \underset{\tilde{X} \in \mathbb{R}^{(n+1) \times (n+1)}}{\text{minimize}} && \left\langle \begin{pmatrix} Q & c \\ c^\top & \cdot \end{pmatrix}, \tilde{X} \right\rangle \\ & \text{subject to} && \left\langle \begin{pmatrix} \cdot & \cdot \\ \cdot & 1 \end{pmatrix}, \tilde{X} \right\rangle = 1, \\ & && \tilde{X} \in \mathcal{C}_{n+1}^* \cap \mathcal{NULC}. \end{aligned} \tag{25}$$

As a quick aside, rewriting the problem in this way does not change the Lagrangian dual problem. To see this, we first write the Lagrangian dual of Problem (25) as

$$\begin{aligned} & \underset{\gamma \in \mathbb{R}, \tilde{M} \in \mathbb{R}^{(n+1) \times (n)}}{\text{maximize}} && \gamma \\ & \text{subject to} && \tilde{M} = \begin{pmatrix} Q & c \\ c^\top & \cdot \end{pmatrix} - \gamma \begin{pmatrix} \cdot & \cdot \\ \cdot & 1 \end{pmatrix}, \\ & && \tilde{M} \in \mathcal{C}_{n+1} + \mathcal{NULC}^* \end{aligned} \tag{26}$$

and notice that  $\mathcal{NULC}^*$  is spanned by

$$\left\{ \begin{pmatrix} A_{i,*}^\top A_{i,*} & -b_i A_{i,*}^\top \\ -b_i A_{i,*} & b_i^2 \end{pmatrix} \right\} \cup \left\{ \begin{pmatrix} -\mathbf{1}_{\{j\}} \mathbf{1}_{\{j\}}^\top & \frac{1}{2} \mathbf{1}_{\{j\}} \\ \frac{1}{2} \mathbf{1}_{\{j\}}^\top & \cdot \end{pmatrix} \right\}. \tag{27}$$

Here, we take care to note that the *Lagrangian* dual may differ from the *conic* dual. In particular, feasibility of (MBQP) is sufficient for ensuring strong duality when  $\tilde{M}$  is optimized over  $(\mathcal{C}^* \cap \mathcal{NULC})^*$

[35, Prop 5.3.9], however it is not guaranteed that  $(C^* \cap \mathcal{NULC})^*$  is equal to  $C + \mathcal{NULC}^*$ —this is the case if and only if  $C + \mathcal{NULC}^*$  is closed.

To establish strong duality, we will first assert that if Problem (MBQP) is feasible with bounded feasible region, then Problem (Hom-CPP) has a nonempty and bounded set of optimal solutions. This follows directly from [8, Corollary 2.6], which states that for all optimal solutions,  $(x^*, X^*)$ , of (Hom-CPP),  $x^*$  must lie within the convex hull of optimal solutions for (MBQP). If the set of optimal solutions for (MBQP) is non-empty and bounded, so is their convex hull. This establishes that the set of optimal solutions of (Hom-CPP) is also non-empty and bounded, allowing us to apply [63, Theorem 1.1].  $\square$

Strong duality means that

$$\max(\text{Hom-COP}) = \min(\text{Hom-CPP}) \quad (28)$$

**Theorem 6.2** (Inhomogeneous Lower Bound). *The optimal objective of Problem (COP) is at least that of Problem (Hom-COP) (i.e.,  $\max(\text{COP}) \geq \max(\text{Hom-COP})$ ).*

*Proof.* We will do this by showing that for each  $(\hat{\mu}, \hat{\lambda}, \hat{\gamma})$  there exists  $(\mu, \lambda, \gamma)$  such that

$$M(\mu, \lambda, \gamma) = \hat{M}(\hat{\mu}, \hat{\lambda}, \hat{\gamma}), \quad (29)$$

and

$$\gamma + \sum_i \mu_i^{(\text{lin})} b_i + \mu_i^{(\text{quad})} b_i^2 = \hat{\gamma}. \quad (30)$$

In other words, any feasible solution for (Hom-COP) can be transformed into a feasible solution for (COP) with equal objective value. To see this, we will suggestively break up  $\gamma = \gamma^{(\text{res})} + \sum_i \gamma_i$  so equation (3) can be expanded as

$$\begin{aligned} M(\mu, \lambda, \gamma) &= \begin{pmatrix} Q & c \\ c^\top & \cdot \end{pmatrix} \\ &\quad - \sum_i \left( \mu_i^{(\text{lin})} \begin{pmatrix} \cdot & \frac{1}{2} A_{i,*}^\top \\ \frac{1}{2} A_{i,*} & \cdot \end{pmatrix} + \mu_i^{(\text{quad})} \begin{pmatrix} A_{i,*}^\top A_{i,*} & \cdot \\ \cdot & \cdot \end{pmatrix} + \gamma_i \begin{pmatrix} \cdot & \cdot \\ \cdot & 1 \end{pmatrix} \right) \\ &\quad - \sum_{j \in B} \lambda_j \begin{pmatrix} -\mathbf{1}_{\{j\}} \mathbf{1}_{\{j\}}^\top & \frac{1}{2} \mathbf{1}_{\{j\}} \\ \frac{1}{2} \mathbf{1}_{\{j\}} & \cdot \end{pmatrix} - \gamma^{(\text{res})} \begin{pmatrix} \cdot & \cdot \\ \cdot & 1 \end{pmatrix} \end{aligned} \quad (31)$$

Then, the proposed  $(\mu, \lambda, \gamma)$  is given by

$$\lambda_j = \hat{\lambda}_j \quad (32)$$

$$\mu_i^{(\text{lin})} = -2b_i \hat{\mu}_i \quad (33)$$

$$\mu_i^{(\text{quad})} = \hat{\mu}_i \quad (34)$$

$$\gamma_i = b_i^2 \hat{\mu}_i \quad (35)$$

$$\gamma^{(\text{res})} = \hat{\gamma} \quad (36)$$

Then, notice that

$$\mu_i^{(\text{lin})} \begin{pmatrix} \cdot & \frac{1}{2} A_{i,*}^\top \\ \frac{1}{2} A_{i,*} & \cdot \end{pmatrix} + \mu_i^{(\text{quad})} \begin{pmatrix} A_{i,*}^\top A_{i,*} & \cdot \\ \cdot & \cdot \end{pmatrix} + \gamma_i \begin{pmatrix} \cdot & \cdot \\ \cdot & 1 \end{pmatrix} \quad (37)$$

$$= -2b_i \hat{\mu}_i \begin{pmatrix} \cdot & \frac{1}{2} A_{i,*}^\top \\ \frac{1}{2} A_{i,*} & \cdot \end{pmatrix} + \hat{\mu}_i \begin{pmatrix} A_{i,*}^\top A_{i,*} & \cdot \\ \cdot & \cdot \end{pmatrix} + b_i^2 \hat{\mu}_i \begin{pmatrix} \cdot & \cdot \\ \cdot & 1 \end{pmatrix} \quad (38)$$

$$= \hat{\mu}_i \left( -2b_i \begin{pmatrix} \cdot & \frac{1}{2} A_{i,*}^\top \\ \frac{1}{2} A_{i,*} & \cdot \end{pmatrix} + \begin{pmatrix} A_{i,*}^\top A_{i,*} & \cdot \\ \cdot & \cdot \end{pmatrix} + b_i^2 \begin{pmatrix} \cdot & \cdot \\ \cdot & 1 \end{pmatrix} \right) \quad (39)$$

$$= \hat{\mu}_i \begin{pmatrix} A_{i,*}^\top A_{i,*} & -b_i A_{i,*}^\top \\ -b_i A_{i,*} & b_i^2 \end{pmatrix} \quad (40)$$



so by matching up terms in the sums, we see that  $M(\mu, \lambda, \gamma) = \hat{M}(\hat{\mu}, \hat{\lambda}, \hat{\gamma})$ . As for the objective value,

$$\gamma + \sum_i \mu_i^{(\text{lin})} b_i + \mu_i^{(\text{quad})} b_i^2 \quad (41)$$

$$= \gamma^{(\text{res})} + \sum_i \mu_i^{(\text{lin})} b_i + \mu_i^{(\text{quad})} b_i^2 + \gamma_i \quad (42)$$

$$= \hat{\gamma} + \sum_i -2b_i^2 \hat{\mu}_i + b_i^2 \hat{\mu}_i + b_i^2 \hat{\mu}_i \quad (43)$$

$$= \hat{\gamma} + \sum_i \hat{\mu}_i (-2b_i^2 + b_i^2 + b_i^2) \quad (44)$$

$$= \hat{\gamma} \quad (45)$$

so for each  $(\hat{\mu}, \hat{\lambda}, \hat{\gamma})$  the proposed  $(\mu, \lambda, \gamma)$  has equal objective value.  $\square$

**Corollary 6.2.1.** *If Problem (MBQP) is feasible with bounded feasible region, then strong duality holds between Problems (CPP) and (COP).*

*Proof.* Theorem shows that  $\max(\text{COP}) \geq \max(\text{Hom-COP})$ . So we have  $\max(\text{Hom-COP}) \leq \max(\text{COP}) \leq \min(\text{CPP}) = \min(\text{Hom-CPP})$ . Combining this with  $\max(\text{Hom-COP}) = \min(\text{Hom-CPP})$  we get

$$\max(\text{Hom-COP}) = \max(\text{COP}) = \min(\text{CPP}) = \min(\text{Hom-CPP}). \quad (46)$$

Thus, strong duality must hold between (COP) and (CPP).  $\square$

## 6.2 Discretizing the copositivity checks

### 6.2.1 Constructing the QUBO

In this section, we will discuss forming the QUBO to approximate the copositivity checks. Formally, instead of solving (10) with feasible region  $\{z \in \mathbb{R}_{\geq 0}^{n+1} \mid \|z\|_{\infty} \leq 1\}$ , we will approximate the feasible region with  $\{0, \frac{1}{K}, \dots, \frac{K-1}{K}, 1\}^{n+1}$ , leading to a quadratic unconstrained integer optimization,

$$\begin{aligned} & \underset{z}{\text{minimize}} && z^{\top} M(\mu, \lambda, \gamma) z \\ & \text{subject to} && z \in \left\{ 0, \frac{1}{K}, \dots, \frac{K-1}{K}, 1 \right\}^{n+1} \end{aligned} \quad (\text{QUIO})$$

For simplicity, assume that  $K = 2^k - 1$  for some  $k \in \mathbb{Z}_{>0}$ . Then Problem (QUIO) is equivalent to minimizing (QUBO), where

$$\hat{M}(\mu, \lambda, \gamma) = \mathcal{D}^{\top} M(\mu, \lambda, \gamma) \mathcal{D} \quad (47)$$

and

$$\mathcal{D} := \begin{pmatrix} \frac{1}{2^0} & \cdots & \frac{1}{2^{k-1}} & 0 & \cdots & 0 & \cdots & 0 & \cdots & 0 \\ 0 & \cdots & 0 & \frac{1}{2^0} & \cdots & \frac{1}{2^{k-1}} & \cdots & 0 & \cdots & 0 \\ \vdots & \vdots & \vdots & \vdots & \vdots & \vdots & \vdots & \vdots & \vdots & \vdots \\ 0 & \cdots & 0 & 0 & \cdots & 0 & \cdots & \frac{1}{2^0} & \cdots & \frac{1}{2^{k-1}} \end{pmatrix}, \quad (48)$$

over the variables  $\hat{z} \in \{0, 1\}^{k(n+1)}$ . This is simply the binary expansion of (QUIO). One could also use a unary expansion at the expense of a larger size expansion and redundancy in the encoding. Additionally, while we have written out a uniform expansion for all variables, it is possible to have a heterogenous discretization scheme. More sophisticated discretization schemes are discussed in depth in [64].

### 6.2.2 Choosing a discretization size

When discretizing the copositivity checks, it is critical to ensure that the discretization size is fine enough. This section provides guidance for choosing a discretization size given a particular QUBO.

Formally, suppose that  $z^\top Mz \geq 0$  for all  $z \in \{0, \frac{1}{K}, \dots, \frac{K-1}{K}, 1\}^n$ . We are interested in lower bounding  $(z + \Delta)^\top M(z + \Delta)$  as a function of  $\|\Delta\|$ . Expanding  $(z + \Delta)^\top M(z + \Delta)$  out we get

$$(z + \Delta)^\top M(z + \Delta) = z^\top Mz + 2\Delta^\top Mz + \Delta^\top M\Delta. \quad (49)$$

So

$$(z + \Delta)^\top M(z + \Delta) \geq -|2\Delta^\top Mz + \Delta^\top M\Delta|. \quad (50)$$

We now want to upper bound  $|2\Delta^\top Mz + \Delta^\top M\Delta|$ .

$$|2\Delta^\top Mz + \Delta^\top M\Delta| = \|2\Delta^\top Mz + \Delta^\top M\Delta\|_\infty \quad (51)$$

$$\leq \|2\Delta^\top Mz\|_\infty + \|\Delta^\top M\Delta\|_\infty \quad (52)$$

$$= 2\|\Delta^\top Mz\|_\infty + \|\Delta^\top M\Delta\|_\infty \quad (53)$$

$$\leq 2\|\Delta\|_\infty \|z\|_\infty \|M\|_\infty + \|\Delta\|_\infty^2 \|M\|_\infty \quad (54)$$

$$\leq (2\|\Delta\|_\infty + \|\Delta\|_\infty^2) \|M\|_\infty. \quad (55)$$

Relating this back to our discretization scheme, notice that any  $\hat{z}$  with  $\|\hat{z}\|_\infty \leq 1$  can be expressed as  $\hat{z} = z + \Delta$  with  $\|\Delta\|_\infty \leq \frac{1}{2K}$  and  $z \in \{0, \frac{1}{K}, \dots, \frac{K-1}{K}, 1\}^n$  (i.e., by rounding). So if the minimum copositivity check is achieved at

$$-\delta = (z + \Delta)^\top M(z + \Delta), \quad (56)$$

the maximum discretization size where this can be undetectable is given by

$$\delta \geq \left(\frac{1}{K} + \frac{1}{4K^2}\right) \|M\|_\infty \quad (57)$$

$$= \left(\left(\frac{1}{2K} + 1\right)^2 - 1\right) \|M\|_\infty \quad (58)$$

$$\frac{\delta}{\|M\|_\infty} + 1 \geq \left(\frac{1}{2K} + 1\right)^2 \quad (59)$$

$$\sqrt{\frac{\delta}{\|M\|_\infty} + 1} - 1 \geq \frac{1}{2K} \quad (60)$$

$$K \geq \frac{1}{2(\sqrt{\frac{\delta}{\|M\|_\infty} + 1} - 1)}. \quad (61)$$

### 6.3 Hyper-parameter optimization

To investigate further speed-ups from turning the simulated annealing parameters, we optimized the number of sweeps using `Hyperopt` [65] with 25 trials for each instance. Figure 8 plots the optimized  $\text{TTT}_{0.99}$  and the  $\text{TTT}_{0.99}$  when `dwave-neal` was run with 100 sweeps. While the optimization produced significant relative improvements for graphs with 10 nodes, the improvement for larger graphs remained marginal, especially in light of the computational overhead required to optimize the parameters. Figure 9 plots the optimal number of sweeps for each problem instance. Generally, the optimal number of sweeps increases with the number of vertices. While graphs of densities  $p = 0.25$  and  $p = 0.75$  require a comparable number of sweeps for graphs of the same size, fewer sweeps are required for graphs with density  $p = 0.5$ .

### 6.4 Illustrative example

In this section, we will walk through a small MBQP to illustrate the translation into the equivalent copositive program. Consider the following mixed-binary optimization problem:

$$\begin{aligned} & \underset{x_1, x_2}{\text{minimize}} && (x_1 \ x_2) \begin{pmatrix} 1 & -1 \\ -1 & \cdot \end{pmatrix} \begin{pmatrix} x_1 \\ x_2 \end{pmatrix} \\ & \text{subject to} && x_1 + x_2 = 1, \\ & && x_1, x_2 \in \mathbb{R}_{\geq 0}. \end{aligned} \quad (\text{Ex-MBPQ})$$

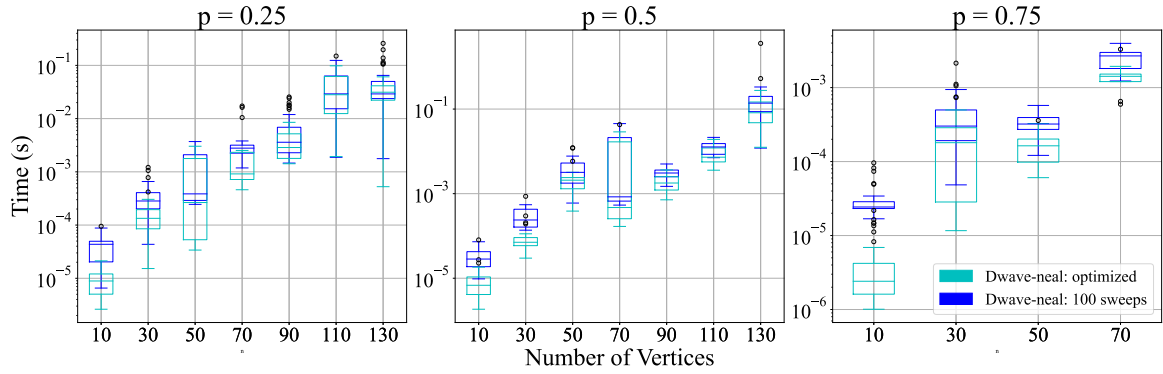


Figure 8: This figure plots the optimized  $TTT_{0.999}$  when `dwave-neal` was run with 100 sweeps. Optimization produces an order of magnitude speed-up for graphs with 10 nodes but does not result in significant speed-ups for larger graphs.

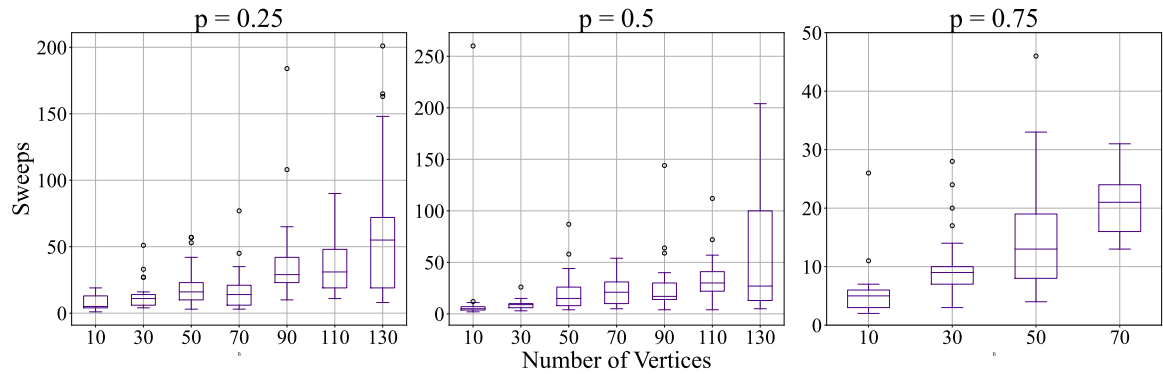


Figure 9: This figure plots the optimal number of sweeps for each of the problem instances. The optimal number of sweeps increases with the graph size. However, graphs of densities  $p = 0.25$  and  $p = 0.75$  require a comparable number of sweeps for graphs of the same size, while fewer sweeps are required for graphs with density  $p = 0.5$

The optimal solution is given by

$$x_1^* = \frac{1}{3}, \quad x_2^* = \frac{2}{3}, \quad (62)$$

which gives an optimal objective value of  $-\frac{1}{3}$ .

The equivalent completely positive program is given by

$$\begin{aligned} & \text{minimize} && \left\langle \begin{pmatrix} 1 & -1 & \cdot \\ -1 & \cdot & \cdot \\ \cdot & \cdot & \cdot \end{pmatrix}, \begin{pmatrix} X & x \\ x^\top & 1 \end{pmatrix} \right\rangle \\ & \text{subject to} && \left\langle \begin{pmatrix} \cdot & \cdot & 1 \\ \cdot & \cdot & 1 \\ 1 & 1 & \cdot \end{pmatrix}, \begin{pmatrix} X & x \\ x^\top & 1 \end{pmatrix} \right\rangle = 2, \\ & && \left\langle \begin{pmatrix} 1 & 1 & \cdot \\ 1 & 1 & \cdot \\ \cdot & \cdot & \cdot \end{pmatrix}, \begin{pmatrix} X & x \\ x^\top & 1 \end{pmatrix} \right\rangle = 1, \\ & && \left\langle \begin{pmatrix} \cdot & \cdot & \cdot \\ \cdot & \cdot & \cdot \\ \cdot & \cdot & 1 \end{pmatrix}, \begin{pmatrix} X & x \\ x^\top & 1 \end{pmatrix} \right\rangle = 1, \\ & && \begin{pmatrix} X & x \\ x^\top & 1 \end{pmatrix} \in \mathcal{C}_3^*. \end{aligned} \quad (\text{Ex-CPP})$$

The optimal solution of (Ex-CPP) is determined by the quadratic expansion of the optimal solution of (Ex-MBPQ) as follows:

$$\begin{pmatrix} X^* & x^* \\ x^{*\top} & 1 \end{pmatrix} = \begin{pmatrix} x_1^* \\ x_2^* \\ 1 \end{pmatrix} \begin{pmatrix} x_1^* & x_2^* & 1 \end{pmatrix} = \begin{pmatrix} 1/9 & 2/9 & 1/3 \\ 2/9 & 4/9 & 2/3 \\ 1/3 & 2/3 & 1 \end{pmatrix} \quad (63)$$

The dual copositive program is given by

$$\begin{aligned} & \text{maximize} && \gamma + 2\mu^{(\text{lin})} + \mu^{(\text{quad})} \\ & && \mu, \lambda, \gamma \\ & \text{subject to} && M(\mu, \lambda, \gamma) \in \mathcal{C}_3 \end{aligned} \quad (\text{Ex-COP})$$

where

$$M(\mu, \lambda, \gamma) = \begin{pmatrix} 1 - \mu^{(\text{quad})} & -1 - \mu^{(\text{quad})} & -\mu^{(\text{lin})} \\ -1 - \mu^{(\text{quad})} & -\mu^{(\text{quad})} & -\mu^{(\text{lin})} \\ -\mu^{(\text{lin})} & -\mu^{(\text{lin})} & -\gamma \end{pmatrix} \quad (64)$$

Figure 10 plots the outer bounding ellipsoid for the first 9 iterations of the copositive cutting plane algorithm (with the ellipsoid method as the cutting-plane algorithm) applied to Problem (Ex-COP). For each iteration, the red dot depicts the test point, and the blue ellipsoid plots the outer bounding ellipsoid at the start of the iteration. The initial ellipsoid is chosen to be a sphere, but as the algorithm progresses, we observe that the outer bounding ellipsoid becomes elongated. This behavior is explained by the fact that the optimal solution set for this particular problem is a line.

## 6.5 Additional plots

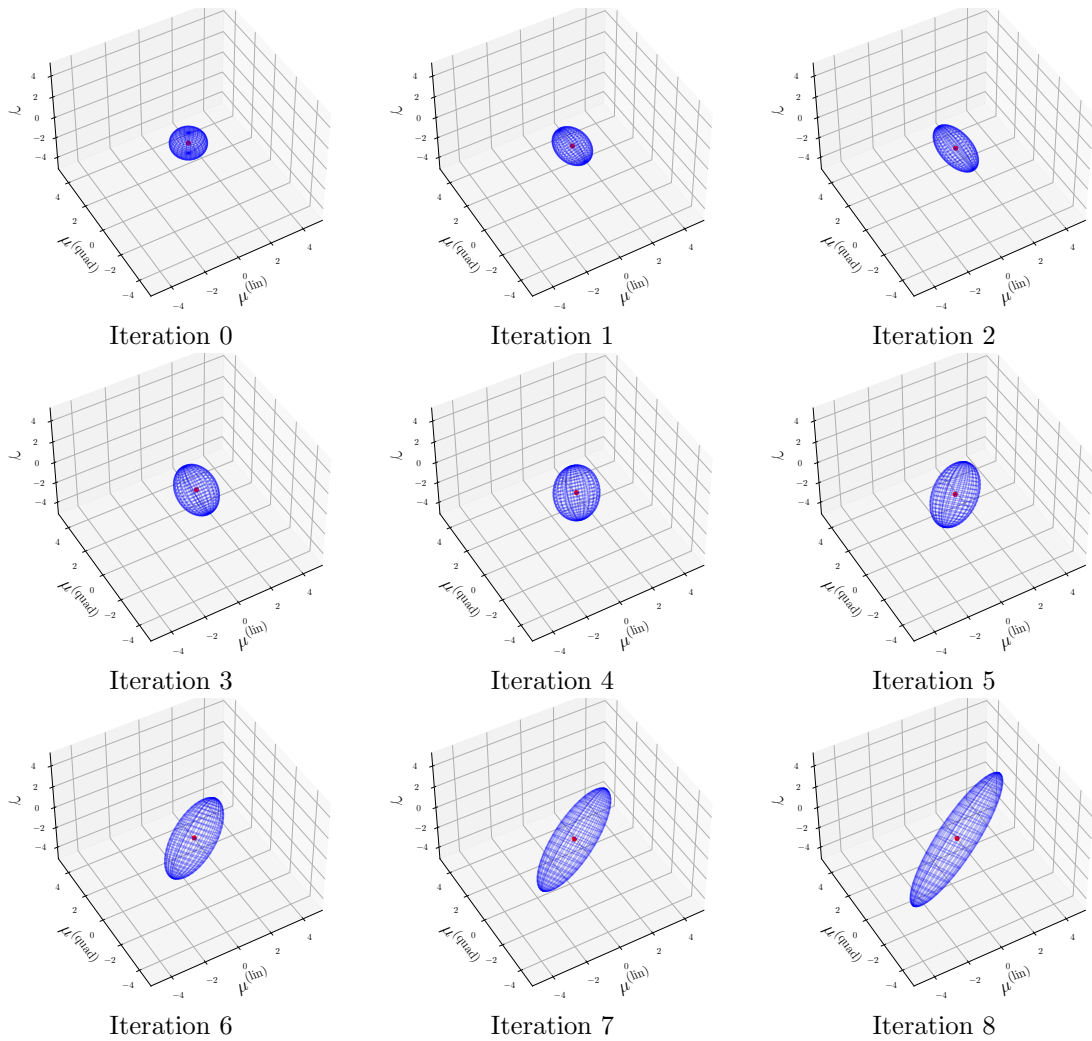


Figure 10: This figure plots the outer bounding ellipsoid for the first 9 iterations of the copositive cutting plane algorithm applied to Problem (Ex-COP). In each plot, the red dot depicts the test point, and the blue ellipsoid plots the outer bounding ellipsoid at the start of the iteration.

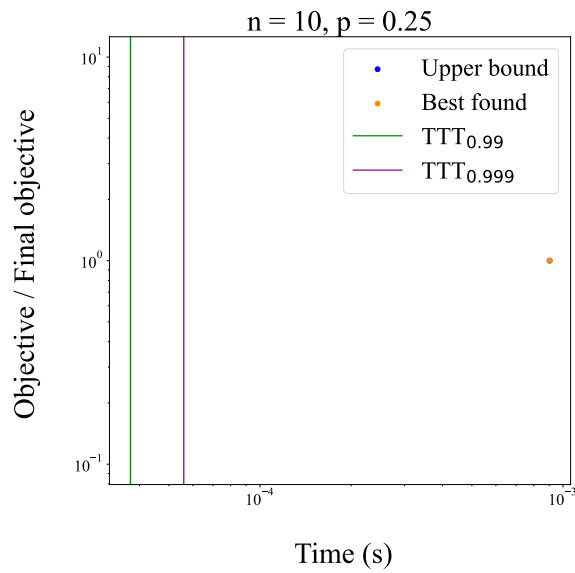


Figure 11: This figure depicts the single instance where **Gurobi** was able to close the gap between upper and lower bounds at the first callback. Even in this case, **TTT<sub>0.999</sub>** with **dwave-neal** is nearly two orders of magnitude faster than **Gurobi**'s solution time.

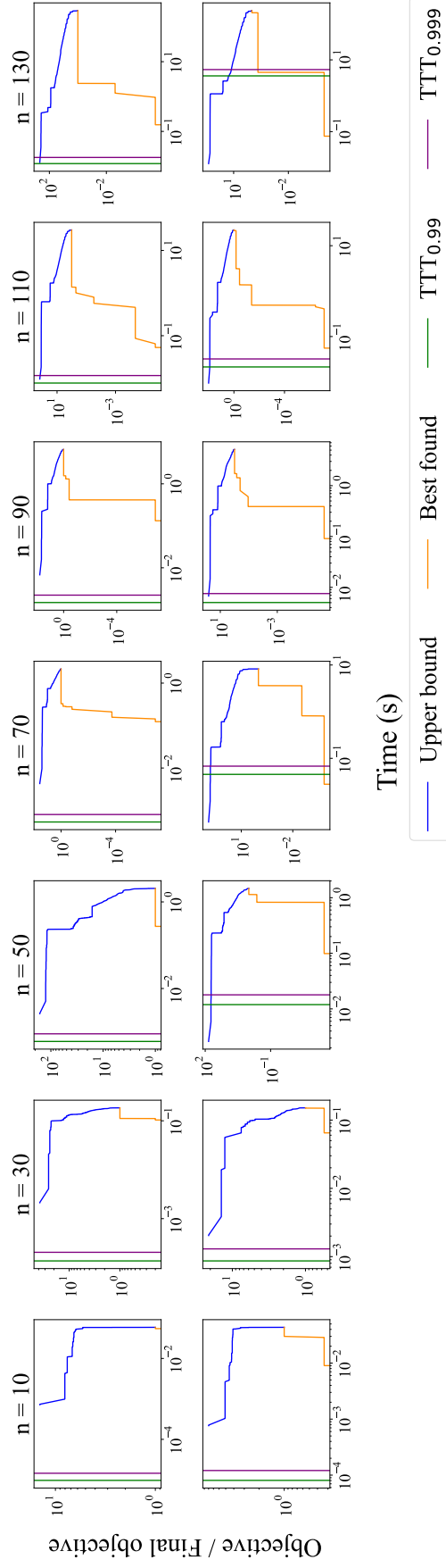


Figure 12: This figure depicts sample trajectories of Gurobi's upper and lower bounds against  $TTT_{0.99}$  and  $TTT_{0.999}$  for edge density  $p = 0.5$ . For each graph size, the top row represents the instance where the ratio between Gurobi's solution time and  $TTT_{0.99}$  is the greatest, and the bottom row represents the instance where the ratio is the smallest—all instances were run with 100 sweeps. In most instances, `dwave-neal` reaches the  $TTT_{0.999}$  confidence before Gurobi even returns a callback (i.e., when the purple line does not intersect either of the blue or orange lines).

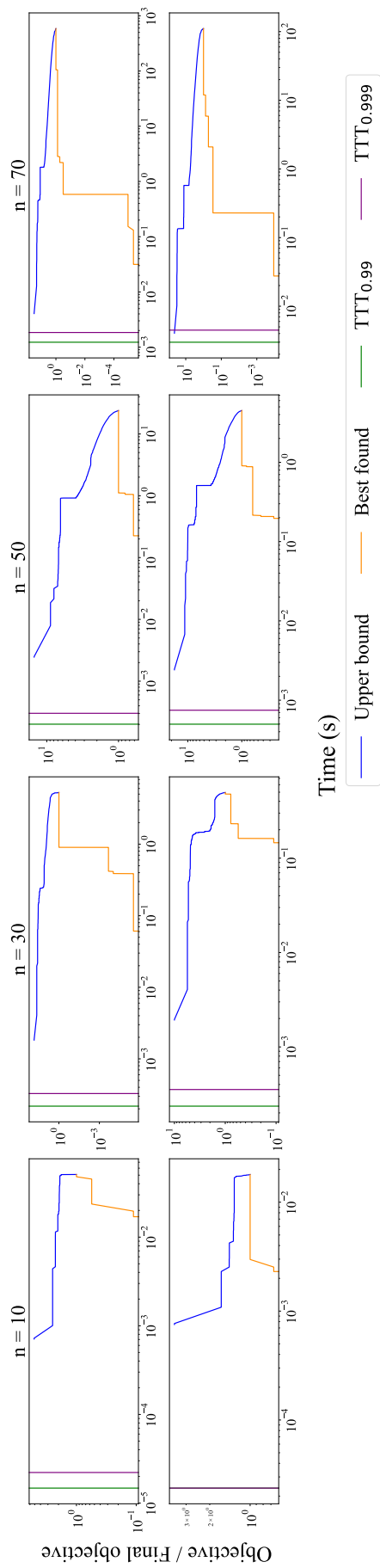


Figure 13: This figure depicts sample trajectories of Gurobi's upper and lower bounds against  $\text{TTT}_{0.99}$  and  $\text{TTT}_{0.999}$  for edge density  $p = 0.75$ . For each graph size, the top row represents the instance where the ratio between Gurobi's solution time and  $\text{TTT}_{0.99}$  is the greatest, and the bottom row represents the instance where the ratio is the smallest—all instances were run with 100 sweeps. In most instances, `dwave-neal` reaches the  $\text{TTT}_{0.999}$  confidence before Gurobi even returns a callback (i.e., when the purple line does not intersect either of the blue or orange lines).



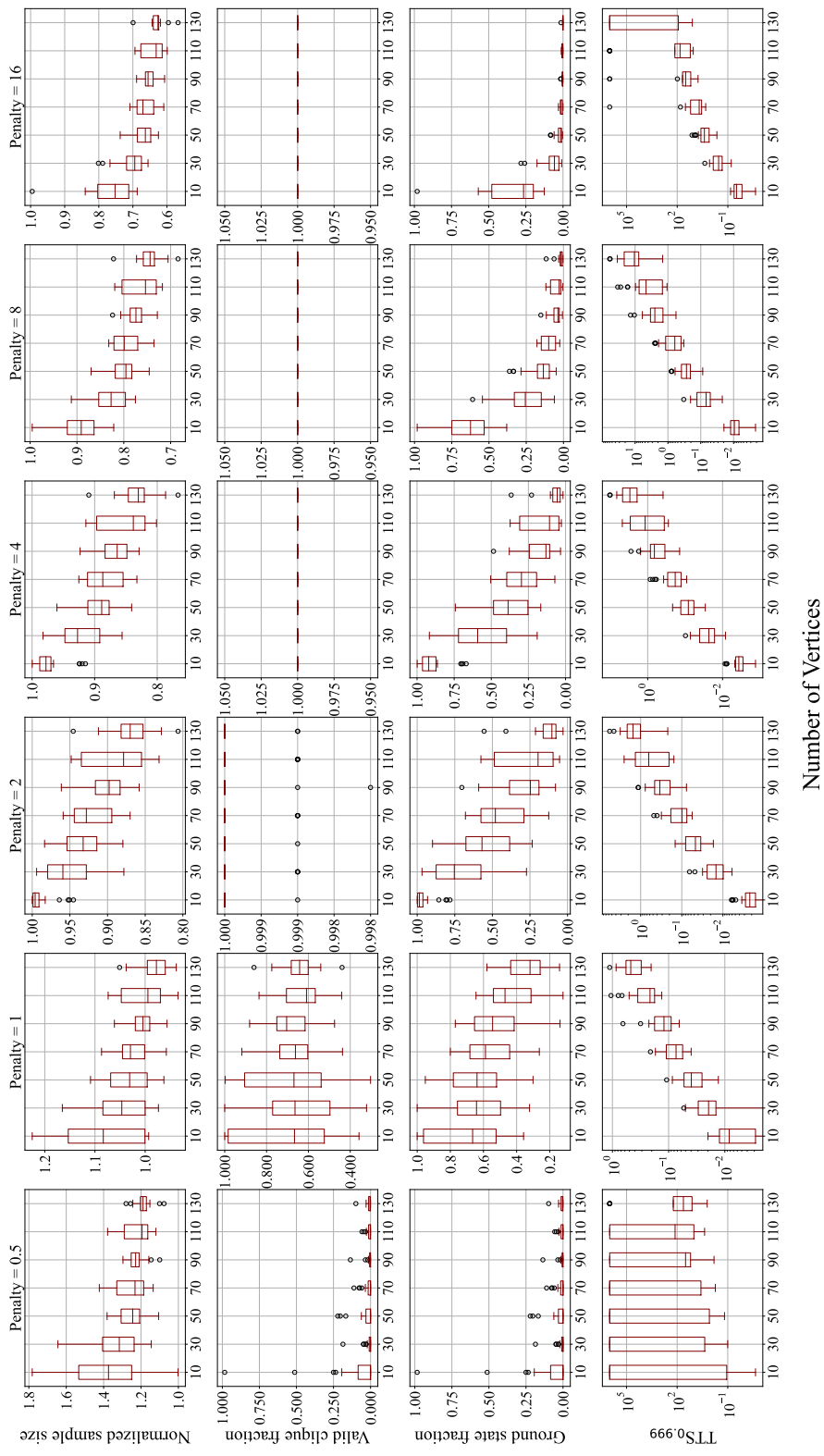


Figure 14: This figure plots the normalized sample size (the size of the returned solution divided by the ground truth maximum clique size) and the fraction of reads that resulted in a valid clique for graph density  $p = 0.5$ . These figures were used to compute the fraction of reads resulting in a ground state solution and the corresponding  $\text{TTS}_{0.999}$  (also plotted). As the penalty weight is increased, the normalized sample size decreases, and the fraction of valid cliques increases. This highlights the delicate trade-off between constraints and the objective in penalty formulations.

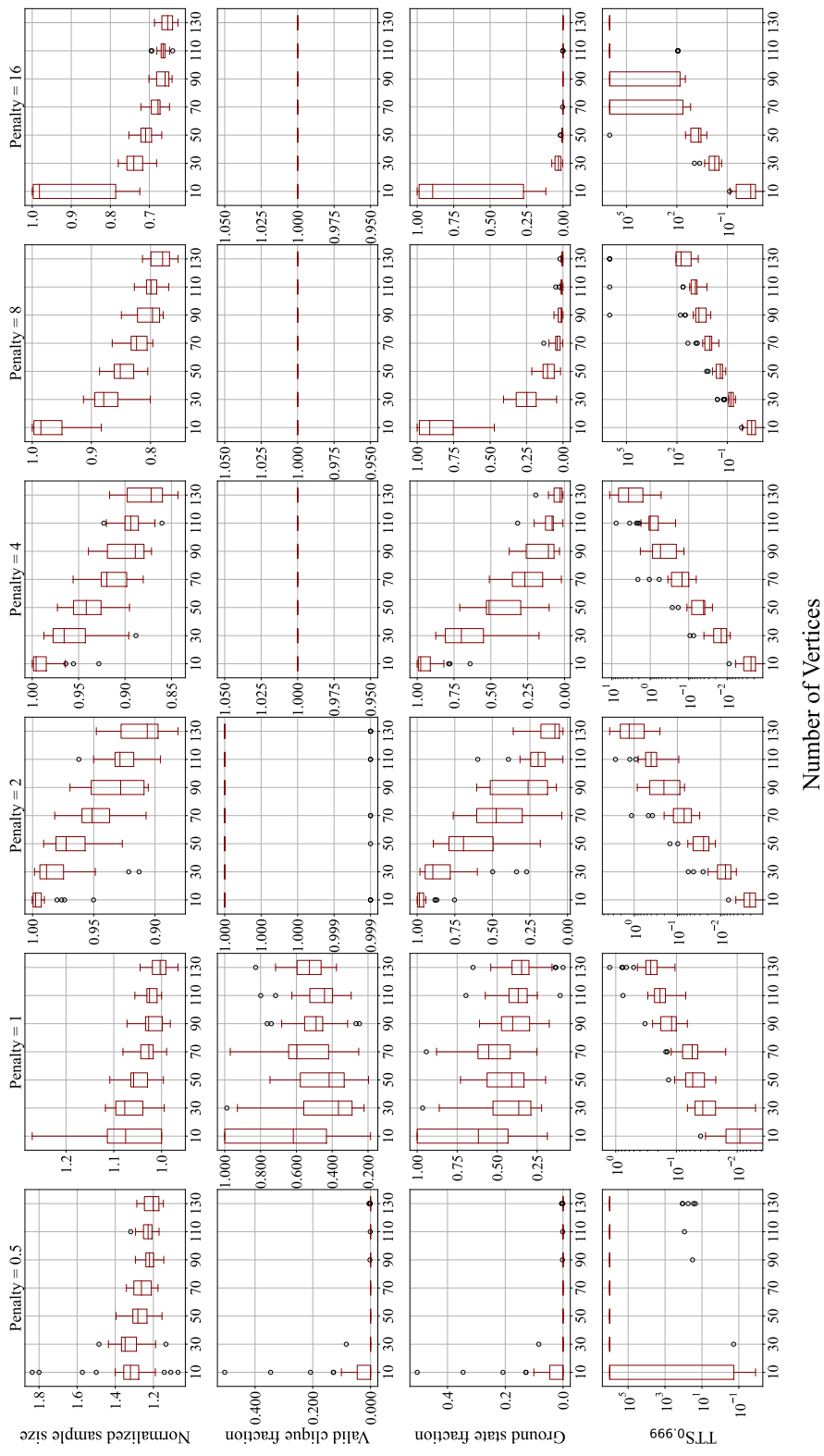


Figure 15: This figure plots the normalized sample size (the size of the returned solution divided by the ground truth maximum clique size) and the fraction of reads that resulted in a valid clique for graph density  $p = 0.75$ . These figures were used to compute the fraction of reads resulting in a ground state solution and the corresponding  $\text{TTS}_{0.999}$  (also plotted). As the penalty weight is increased, the normalized sample size decreases, and the fraction of valid cliques increases. This highlights the delicate trade-off between constraints and the objective in penalty formulations.